[redacted]

Copy 230
RM L55D20

NACA RM L55D20

TECH LIBRARY KAFB, NM
0144121

7613

NACA

RESEARCH MEMORANDUM

EXPERIMENTAL STATIC AERODYNAMIC FORCES AND MOMENTS AT LOW SPEED ON A MISSILE MODEL DURING SIMULATED LAUNCHING FROM THE 25-PERCENT-SEMISPAN AND WING-TIP LOCATIONS OF A 45° SWEPTBACK WING-FUSELAGE COMBINATION

By William J. Alford, Jr., H. Norman Silvers,
and Thomas J. King, Jr.

Langley Aeronautical Laboratory
Langley Field, Va.

[redacted]

[redacted] contains information affecting the National Defense of the United States within the meaning of the espionage laws, Title 18, U.S.C., [redacted] transmission or revelation of which in any [redacted] person is prohibited by law.

NATIONAL ADVISORY COMMITTEE
FOR AERONAUTICS
WASHINGTON
May 25, 1955

[redacted]

TECH LIBRARY KAFB, NM
0144121

 [redacted]

NATIONAL ADVISORY COMMITTEE FOR AERONAUTICS

RESEARCH MEMORANDUM

EXPERIMENTAL STATIC AERODYNAMIC FORCES AND MOMENTS AT LOW SPEED ON A MISSILE MODEL DURING SIMULATED LAUNCHING FROM THE 25-PERCENT-SEMISPAN AND WING-TIP LOCATIONS OF A 45° SWEPTBACK WING-FUSELAGE COMBINATION

By William J. Alford, Jr., H. Norman Silvers,
and Thomas J. King, Jr.

SUMMARY

An investigation was made at low speed in the Langley 300 MPH 7- by 10-foot tunnel to determine the static aerodynamic forces and moments on a missile model during simulated launching from the 25-percent-semispan and wing-tip locations of a wing-fuselage combination having a 45° sweptback wing. The results indicated that, when the missile was mounted under the wing at the 25-percent-semispan location, changes in chordwise position generally produced large changes in missile forces and moments. As the angle of attack was increased, the effects on the missile forces and moments induced by the wing-fuselage combination also increased. The effects induced by the fuselage, when the wing of the wing-fuselage combination was removed, were much less severe than those induced by the wing-fuselage combination. When the missile was located symmetrically at the wing-tip location, the missile forces and moments were comparable in magnitude to those of the missile when at the inboard underwing location, but were considerably less erratic with changes in chordwise position. However, because of the presence of the wing-tip vortex, the missile rolling moments were considerably larger for the tip location.

INTRODUCTION

The National Advisory Committee for Aeronautics is conducting investigations to determine the nature and origin of the mutual interference effects experienced by various combinations of wing-fuselage models and external stores. Previous investigations (refs. 1 to 3) have shown the

[redacted]

[redacted]

existence of these generally objectionable interference effects and reference 4 has shown that they are primarily due, at low speed, to the nonuniform field of flow generated in the vicinity of the model. The result of an investigation of the forces and moments of the missile of this investigation at the midsemispan location of the wing-fuselage combination has been reported in reference 5. Reference 6 has reported the results of an investigation of the force and moment characteristics of a canard missile at the midsemispan and wing-tip locations of the wing-fuselage combination of this investigation.

The present paper presents the low-speed static aerodynamic force and moment characteristics of the missile during simulated launching from the 25-percent-semispan and wing-tip locations of a 45° sweptback wing of a wing-fuselage combination. Also presented are static force and moment measurements on the missile located at the 25-percent-semispan location with the wing of the wing-fuselage combination removed. The effects of a wing fence at the 60-percent-semispan station on the missile forces and moments when located at the wing-tip location were investigated. The isolated missile characteristics as determined from breakdown tests and the lift characteristics of the wing-fuselage combination are presented for orientation.

SYMBOLS

N	missile normal force, lb
m	missile pitching moment, ft-lb
A	missile axial force, lb
Y	missile side force, lb
n	missile yawing moment, ft-lb
l	missile rolling moment, ft-lb
C_N	missile normal-force coefficient, $\frac{N}{qS_m}$
C_A	missile axial-force coefficient, $\frac{A}{qS_m}$

[redacted]

C_m	missile pitching-moment coefficient, $\frac{m}{qS_m\bar{c}_m}$
C_Y	missile side-force coefficient, $\frac{Y}{qS_m}$
C_n	missile yawing-moment coefficient, $\frac{n}{qS_mb_m}$
C_l	missile rolling-moment coefficient, $\frac{l}{qS_mb_m}$
C_{L_W}	lift coefficient of wing-fuselage combination, $\frac{Lift}{qS}$
q	free-stream dynamic pressure, lb/sq ft
V_o	free-stream velocity, ft/sec
S_m	exposed missile-wing area of two panels, 0.046 sq ft
S	total wing area of wing-fuselage combination, 6.25 sq ft
b_m	span of missile wing, 0.415 ft
b	span of wing-fuselage combination, 5 ft
c	local wing chord, ft
$\bar{c}_m$	mean aerodynamic chord of exposed missile-wing area (two panels), 0.189 ft
x	chordwise distance from leading edge of the local wing chord to the missile center of gravity (positive rearward), ft
y	spanwise distance from fuselage center line to missile center line (positive right), ft
z	vertical distance from wing-chord plane (positive up), ft
d_m	diameter of missile body, 1.08 in.
α	angle of attack, deg

MODELS AND APPARATUS

The wing of the wing-fuselage combination used as the test vehicle had a quarter-chord sweepback of 45°, an aspect ratio of 4.0, a taper ratio of 0.3, and NACA 65A006 airfoil sections parallel to the fuselage center line. A wing fence, designed to delay the loss of load over the tip portion of the wing, was employed for one chordwise location of the missile when located at the wing tip. The fence was located at the wing 60-percent-semispan station as shown in the two-view drawing of the test setup (fig. 1). The fuselage (with ordinates given in table I) consisted of an ogival nose section, a cylindrical center section, and a truncated tail cone. The missile model used in this investigation employed an inline cruciform arrangement of its wing and tail, with a fuselage that consisted of an ogival nose and cylindrical after section, and is shown in figure 1 as part of the test setup. Details of the missile model are shown in figure 2.

The missile was internally instrumented with a six-component strain-gage balance and was supported from the rear of the wing-fuselage combination by a sting that was adjustable in the longitudinal, lateral, and vertical planes (fig. 1). Two lateral locations of the missile model were employed during this investigation (0.25b/2 and 1.02b/2). At the inboard location, the longitudinal axis of the missile was 13 percent of the local wing chord below the wing-chord plane. At the wing-tip location, the missile was symmetrically mounted with respect to the wing-chord plane. In each lateral location, the missile was translated longitudinally through a range of chordwise locations. For several of the chordwise locations investigated at the inboard station, the wing of the wing-fuselage combination was removed.

TESTS

The tests were made in the Langley 300 MPH 7- by 10-foot tunnel at a velocity of 100 miles per hour, a dynamic pressure of 25.5 pounds per square foot, and a Reynolds number of 0.92×10^6 per foot of a typical dimension. Six-component force and moment measurements were made on the missile model through an angle-of-attack range that generally extended from -8° to 28°.

The missile was tested under the left wing and at the left wing tip of the test vehicle, which was inverted so as to avoid support-strut interference (fig. 3). The directions of positive forces and moments about the missile center of gravity are as shown in figure 4.

CORRECTIONS AND ACCURACY

Blockage corrections were applied to the dynamic pressure by use of reference 7, and jet-boundary corrections, calculated by the method of reference 8, have been applied to the angle of attack. In addition, a correction of 0.2° angle of attack was applied to account for the tunnel free-stream misalinement angle.

A study of the missile model strain-gage balance calibrations and general repeatability of the test data indicated that the accuracy levels of the various force and moment coefficients are approximately as follows:

Component	Accuracy
C_N	±0.020
C_m	±0.020
C_Y	±0.020
C_n	±0.010
C_l	±0.005
C_A	±0.005

RESULTS AND DISCUSSION

The static aerodynamic characteristics of the isolated missile at low speed, as determined from breakdown tests, are presented in figure 5. These data include only the forces and moments in the longitudinal plane, that is, normal forces and pitching moments; but, because of the model symmetry, the results also are applicable as side forces and yawing moments due to sideslip if the appropriate nondimensionalizing parameters are considered. (See the coefficients in "Symbols.") The basic data of the missile model, when in proximity to the wing-fuselage combination, are presented as a function of angle of attack in figures 6 to 8 and are presented as a function of chordwise position in figures 9 and 10. The lift characteristics of the isolated wing-fuselage combination are presented for orientation in figure 11.

Figures 6 and 9 indicate that changes in chordwise position of the missile at the 25-percent-semispan location produce large changes in the forces and moments of the missile in both the longitudinal and lateral planes when compared with the isolated missile characteristics. These large forces and moments are induced on the missile because of the nonuniform flow field generated by the airplane model and can be explained by a consideration of the flow characteristics similar to those reported

in reference 4. For instance, when the missile center of gravity is located rearward of the wing leading edge ($x/c = 0.60$, fig. 6(a)) at positive angles of attack, the missile wings are operating in a region of downwash. The tail, however, is in a region of slightly higher angularity. The net result is a decreased normal force and a nose-down pitching moment. (See fig. 6(a).) As the missile is moved forward (center of gravity moved to $x/c = 0.31$), the missile wings are still in a downwash field; but now the angularity at the tail is also decreased, giving a normal force less than that for the isolated missile, and because of a loss of tail effectiveness, a nose-up moment results. Further forward movement (fig. 6(b)) causes the missile wings to operate in regions of severe upwash while the tail is at lower values and, hence, the normal force is increased and the pitching moment is nose-up, except for the last missile center-of-gravity location ($x/c = 0.72$) where the tail has entered into the upwash region and a nose-down moment results.

A similar analysis can be effected for the missile lateral characteristics. Reference 4 indicates that large local sidewash or sideslip angularities are generated beneath the wings of the wing-fuselage combination, even at zero angle of sideslip. The maximum values of these local sideslip angles occur near the leading edge of the local wing chord and are in an outboard direction (toward the wing tip) for positive angles of attack; thus, negative side forces are induced (force directed toward the tip). The yawing moment is at first nose outboard when the missile wings are in the higher angular region (fig. 6(a)) and then nose inboard when the missile tail enters the maximum sidewash region as seen in figure 6(b).

The preceding discussion has dealt with positive angles of attack for which, at this speed, the flow beneath the wings is essentially of a potential nature. In the case of the negative angles of attack, however, a condition for which, due to airplane-model symmetry, the results can be assumed to apply to a missile mounted above the wing, the flow characteristics are much more severe and, hence, the induced missile forces and moments are larger and more erratic (figs. 6, 9(a), and 9(b)).

In general, the effect of increasing the angle of attack was to increase the missile forces and moments. This can be explained, from reference 4, by the increase in wing-fuselage circulation strength which results in increased downwash and sidewash angularity fields in conjunction with a nonuniform dynamic-pressure field. Reducing the angle of attack to zero did not, however, eliminate the induction effects since the effects of wing sweep and finite thickness still generate objectionable characteristics (figs. 6 and 9(c)).

It would be expected (it has been shown in ref. 5 for the missile located at the midsemispan location) that the wing-fuselage induction effects would diminish as the missile was moved sufficiently far, either longitudinally or vertically, from the wing-fuselage combination. This was not possible in the present investigation since the physical limitations of the missile supporting members prevented studies in these regions.

A comparison of the results obtained on the missile in the presence of the fuselage (fig. 7) with the results obtained on the missile in the presence of the wing-fuselage combination (fig. 6) is presented in figure 9. This comparison indicates that the wing-fuselage combination induces the larger changes in missile forces and moments when the missile is translated longitudinally at the 25-percent-semispan location.

With the missile mounted symmetrically at the wing tip (figs. 8 and 10) the normal forces are of the same order of magnitude, and the side forces are slightly greater than the forces that exist with the missile located at the inboard underwing locations (figs. 6 and 9). The pitching and yawing moments are somewhat lessened and both the moments and forces are considerably less erratic than at the inboard location as the chordwise position of the missile is changed. The missile rolling moment is an exception, however, and was greatly increased in regions near the wing-tip leading edge because of the effect of the wing-tip vortex.

The wing fence (fig. 8) had a negligible effect on the forces and moments acting on the missile at the wing tip when the missile was mounted in the one chordwise location investigated using the fence.

CONCLUSIONS

The results of an investigation at low speed of the static aerodynamic forces and moments on a missile model during simulated launching from the 25-percent-semispan and wing-tip locations of a wing-fuselage combination having a 45° sweptback wing indicate the following conclusions:

1. When the missile was mounted under the wing at the 25-percent-semispan location, changes in chordwise position generally produced large changes in missile forces and moments. As the angle of attack was increased, the effects on the missile forces and moments induced by the wing-fuselage combination also increased.

2. The effects induced by the fuselage, when the wing of the wing-fuselage combination was removed, were much less severe than those induced by the wing-fuselage combination.

3. When the missile was located symmetrically at the wing tip, the missile forces and moments were comparable in magnitude to those of the missile when located at the inboard underwing location, but were considerably less erratic with changes in chordwise position. Because of the presence of the wing-tip vortex, however, the missile rolling moments were considerably larger for the tip location.

Langley Aeronautical Laboratory,
National Advisory Committee for Aeronautics,
Langley Field, Va., March 25, 1955.

REFERENCES

1. Alford, William J., Jr., and Silvers, H. Norman: Investigation at High Subsonic Speeds of Finned and Unfinned Bodies Mounted at Various Locations From the Wings of Unswept- and Swept-Wing—Fuselage Models, Including Measurements of Body Loads. NACA RM L54B18, 1954.

2. Silvers, H. Norman, and King, Thomas J., Jr.: Investigation at High Subsonic Speed of Bodies Mounted From the Wing of an Unswept-Wing—Fuselage Model, Including Measurements of Body Loads. NACA RM L52J08, 1952.

3. Silvers, H. Norman, and Alford, William J., Jr.: Investigation at High Subsonic Speeds of the Effect of Adding Various Combinations of Missiles on the Aerodynamic Characteristics of Sweptback and Unswept Wings Combined With a Fuselage. NACA RM L54D20, 1954.

4. Alford, William J., Jr., Silvers, H. Norman, and King, Thomas J., Jr.: Preliminary Low-Speed Wind-Tunnel Investigation of Some Aspects of the Aerodynamic Problems Associated With Missiles Carried Externally in Positions Near Airplane Wings. NACA RM L54J20, 1954.

5. Alford, William J., Jr., Silvers, H. Norman, and King, Thomas J., Jr.: Experimental Aerodynamic Forces and Moments at Low Speed of a Missile Model During Simulated Launching From the Midsemispan Location of a 45° Sweptback Wing-Fuselage Combination. NACA RM L54K11a, 1955.

6. Alford, William J., Jr.: Experimental Static Aerodynamic Forces and Moments at Low Speed on a Canard Missile During Simulated Launching From the Midsemispan and Wing-Tip Locations of a 45° Sweptback Wing-Fuselage Combination. NACA RM L55A12, 1955.

7. Herriot, John G.: Blockage Corrections for Three-Dimensional-Flow Closed-Throat Wind Tunnels, With Consideration of the Effect of Compressibility. NACA Rep. 995, 1950. (Supersedes NACA RM A7B28.)

8. Gillis, Clarence L., Polhamus, Edward C., and Gray, Joseph L., Jr.: Charts for Determining Jet-Boundary Corrections for Complete Models in 7- by 10-Foot Closed Rectangular Wind Tunnels. NACA WR L-123, 1945. (Formerly NACA ARR L5G31.)

TABLE I

FUSELAGE ORDINATES

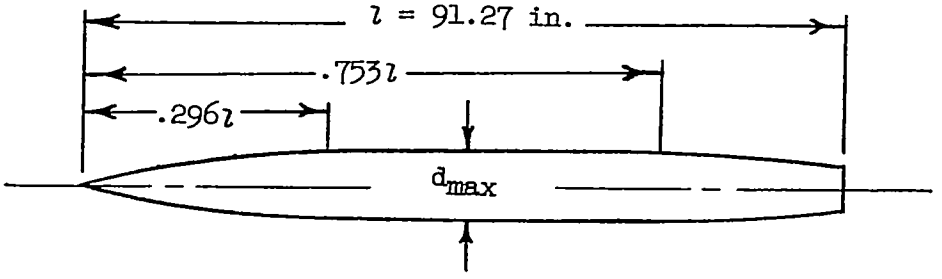

Ordinates, percent length	
Station	Radius
0	0
3.28	.91
6.57	1.71
9.86	2.41
13.15	3.00
16.43	3.50
19.72	3.90
23.01	4.21
26.29	4.43
29.58	4.57
75.34	4.57
76.69	4.54
79.98	4.38
83.26	4.18
86.55	3.95
89.84	3.72
93.13	3.49
96.41	3.26
100.00	3.02

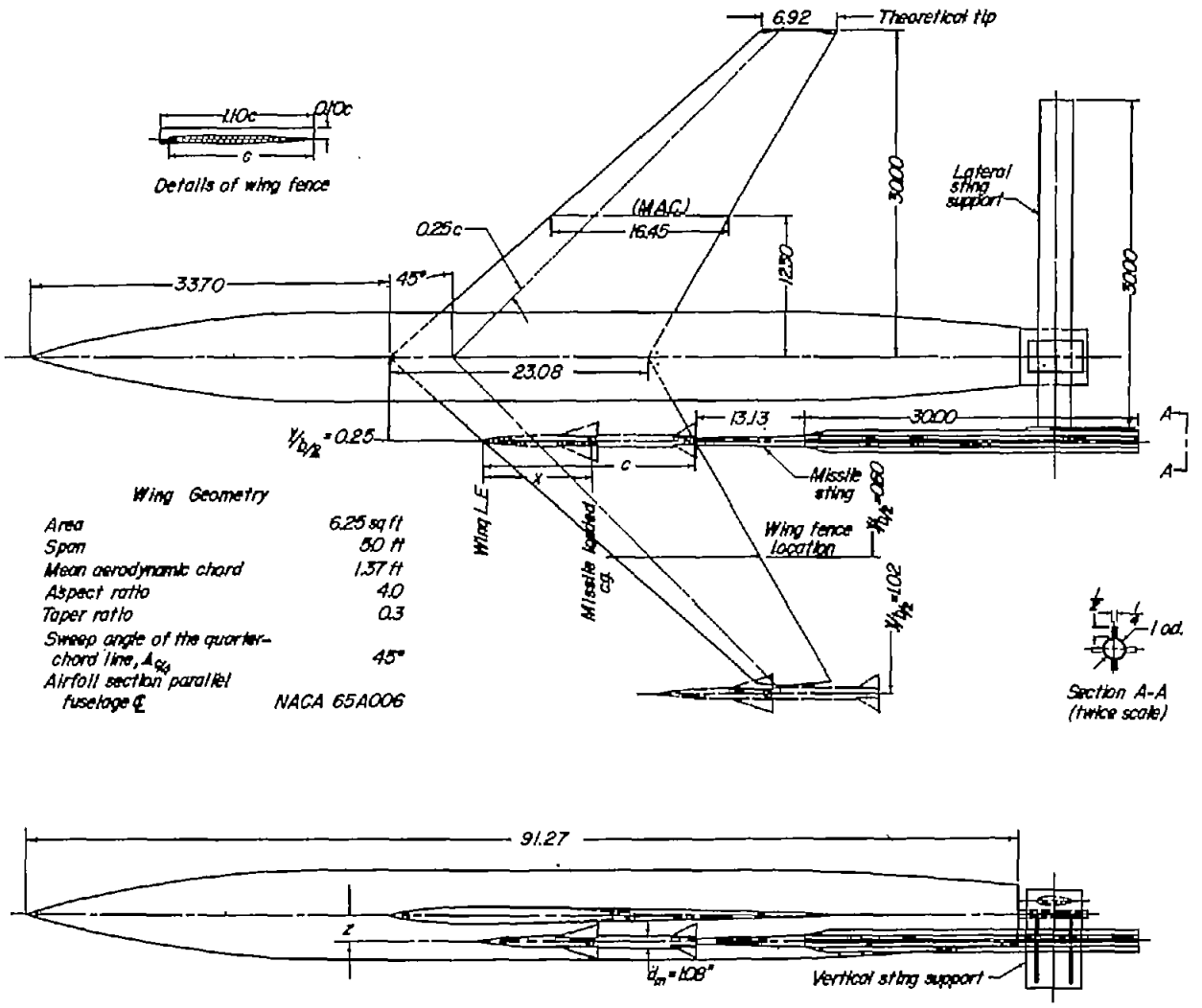

Figure 1.- Test setup showing the missile in test locations. All dimensions are in inches.

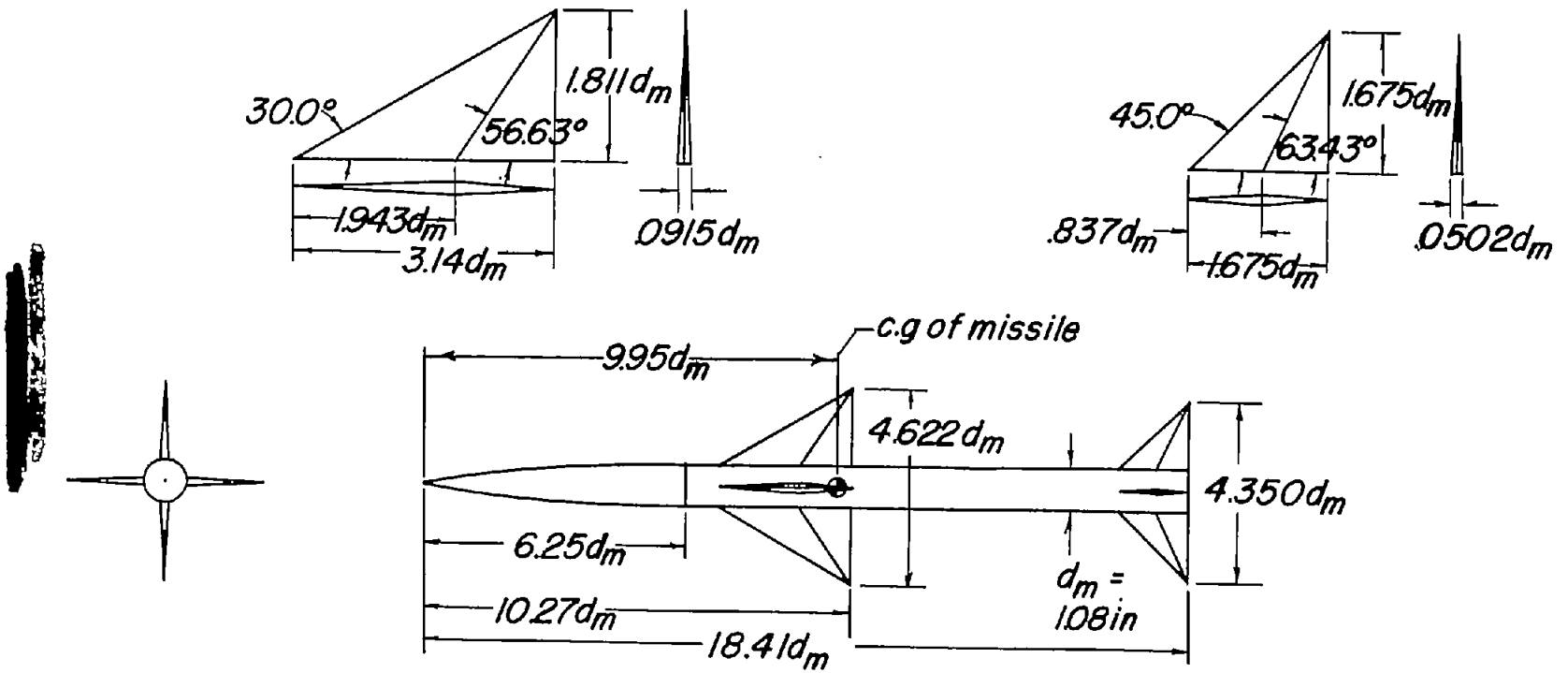

Figure 2.- Drawing of missile model showing general proportions.

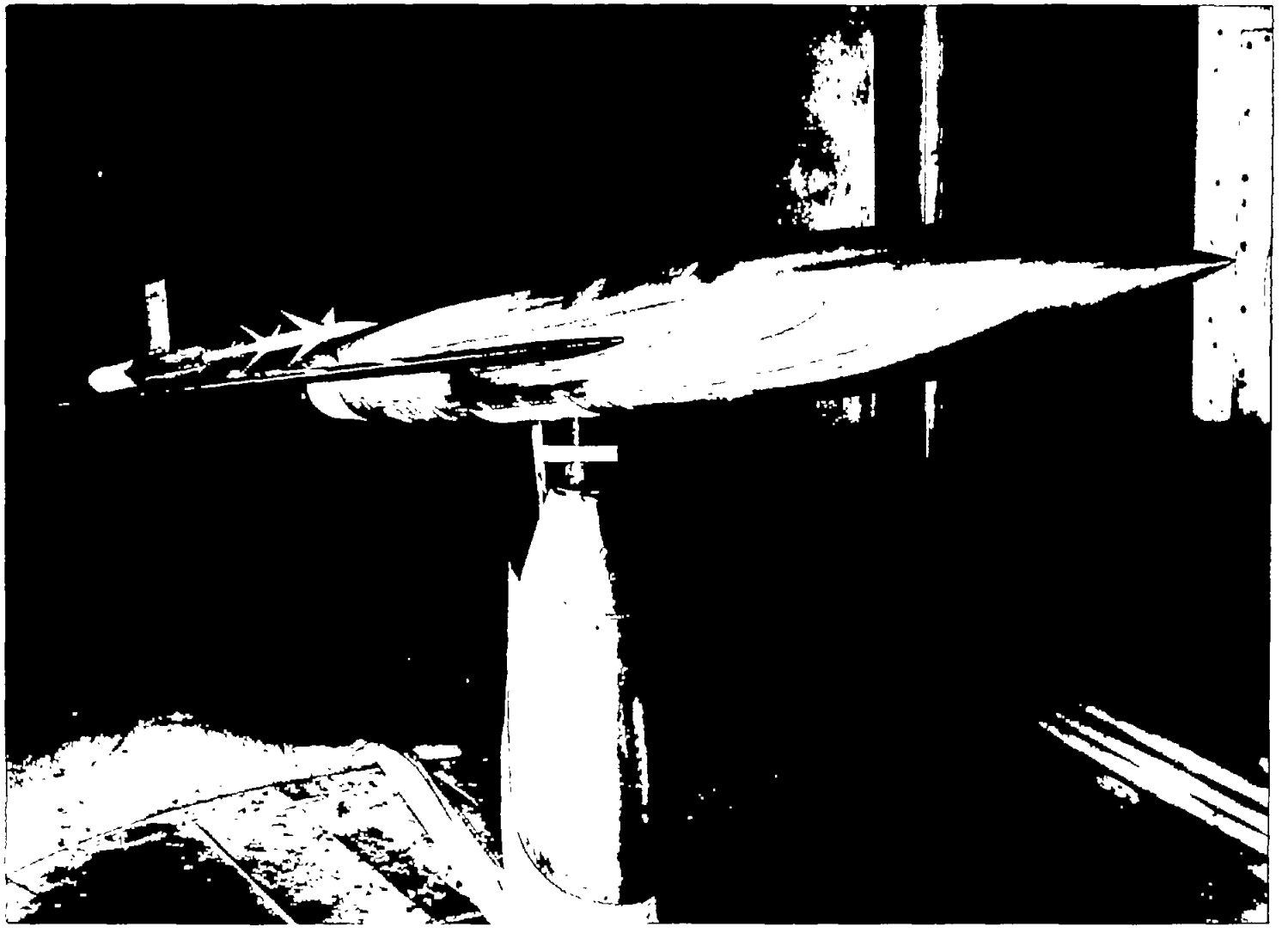

L-82628

Figure 3.- Photograph of the test setup showing the missile installed.

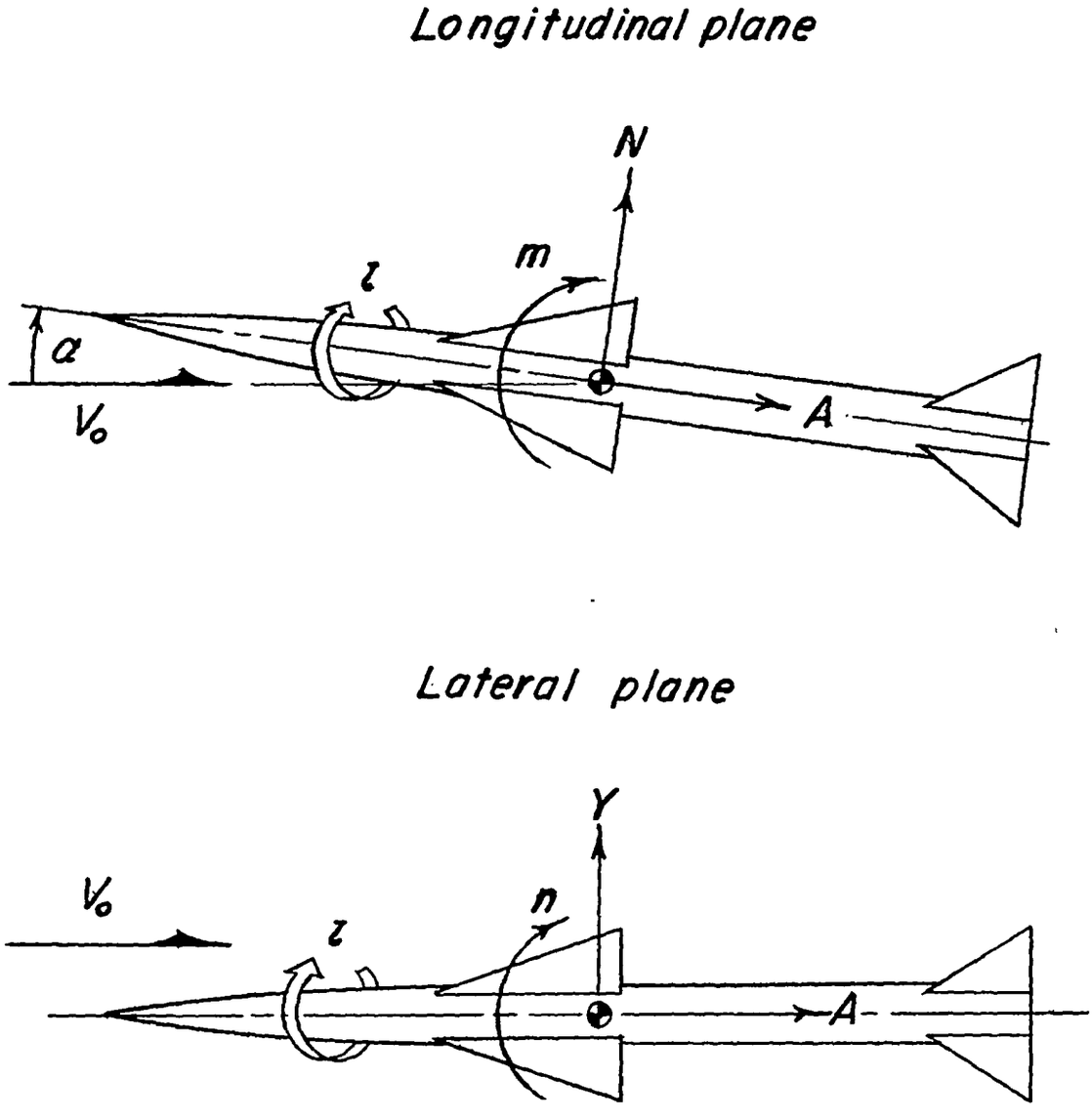

Figure 4.- Positive directions of forces and moments as measured on the missile.

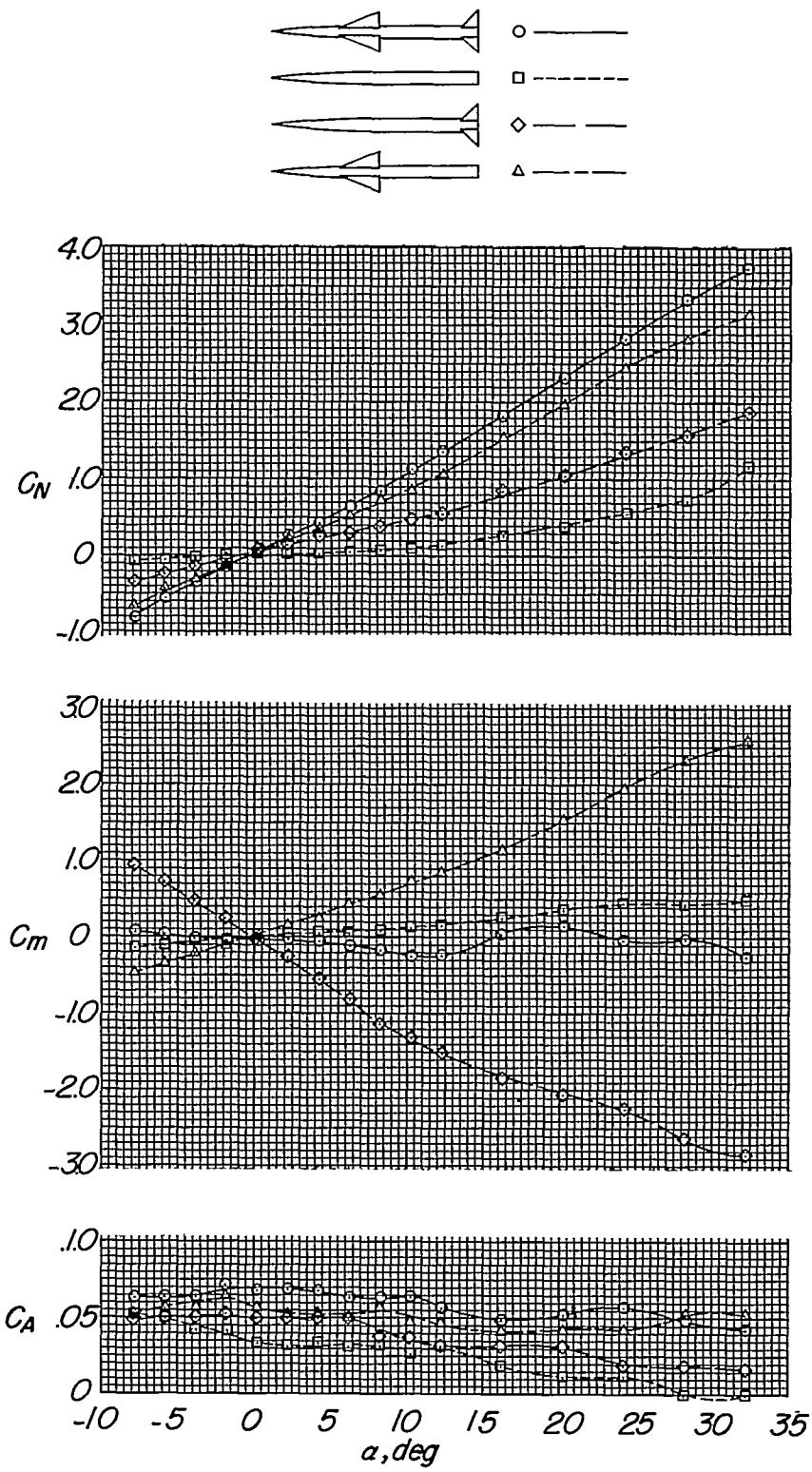

Figure 5.- Isolated-missile and missile-component characteristics.

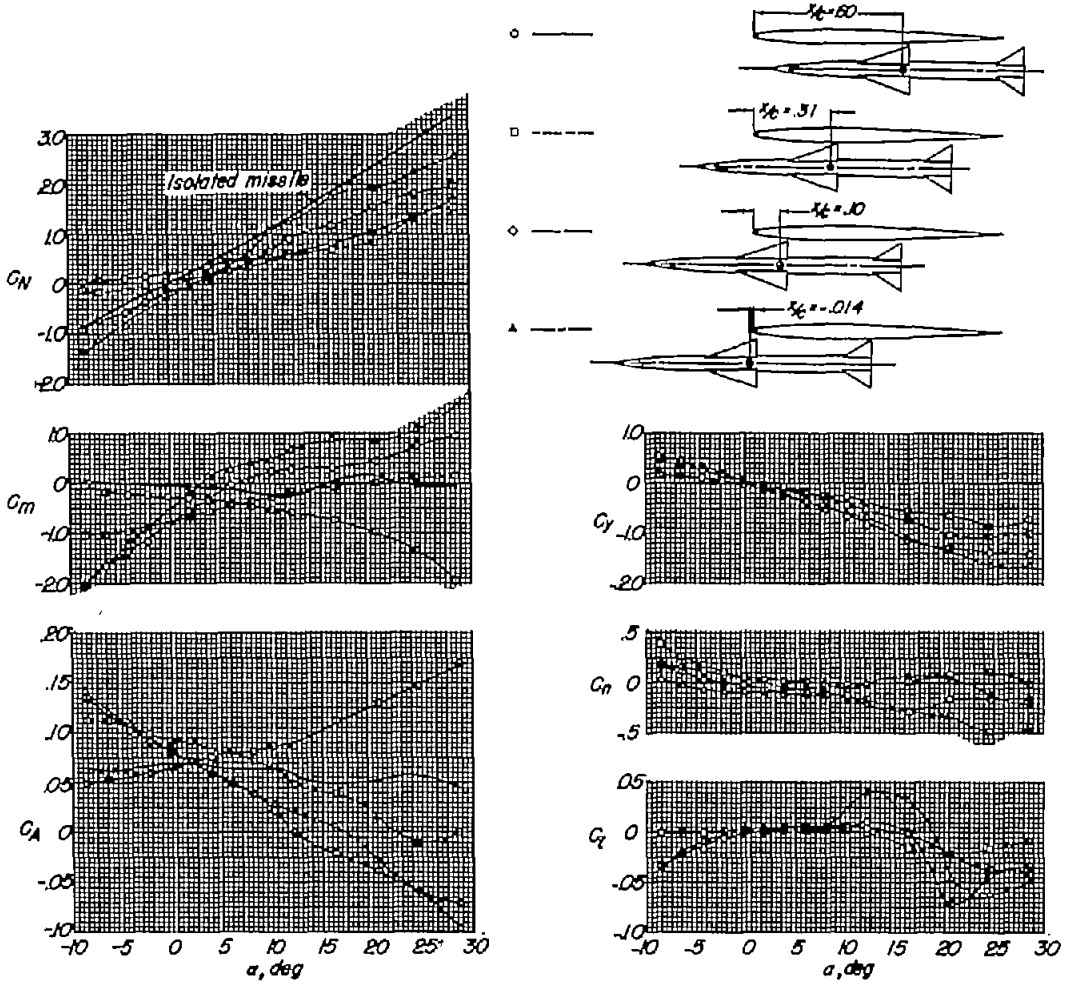

(a) x/c = 0.60 to x/c = -0.014.

Figure 6.- Missile aerodynamic forces and moments when at the 25-percent-semispan location of the wing-fuselage combination.

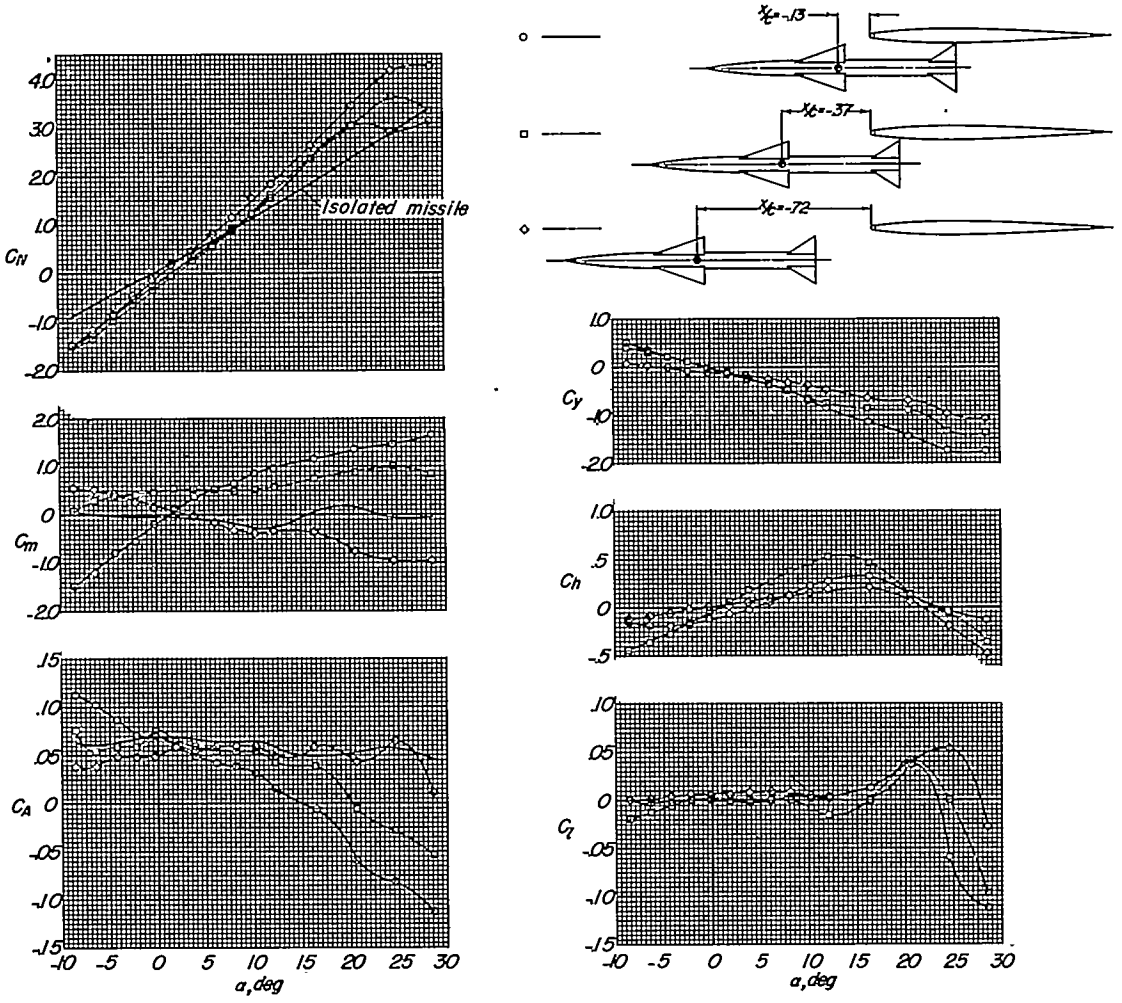

(b) x/c = -0.13 to x/c = -0.72.

Figure 6.- Concluded.

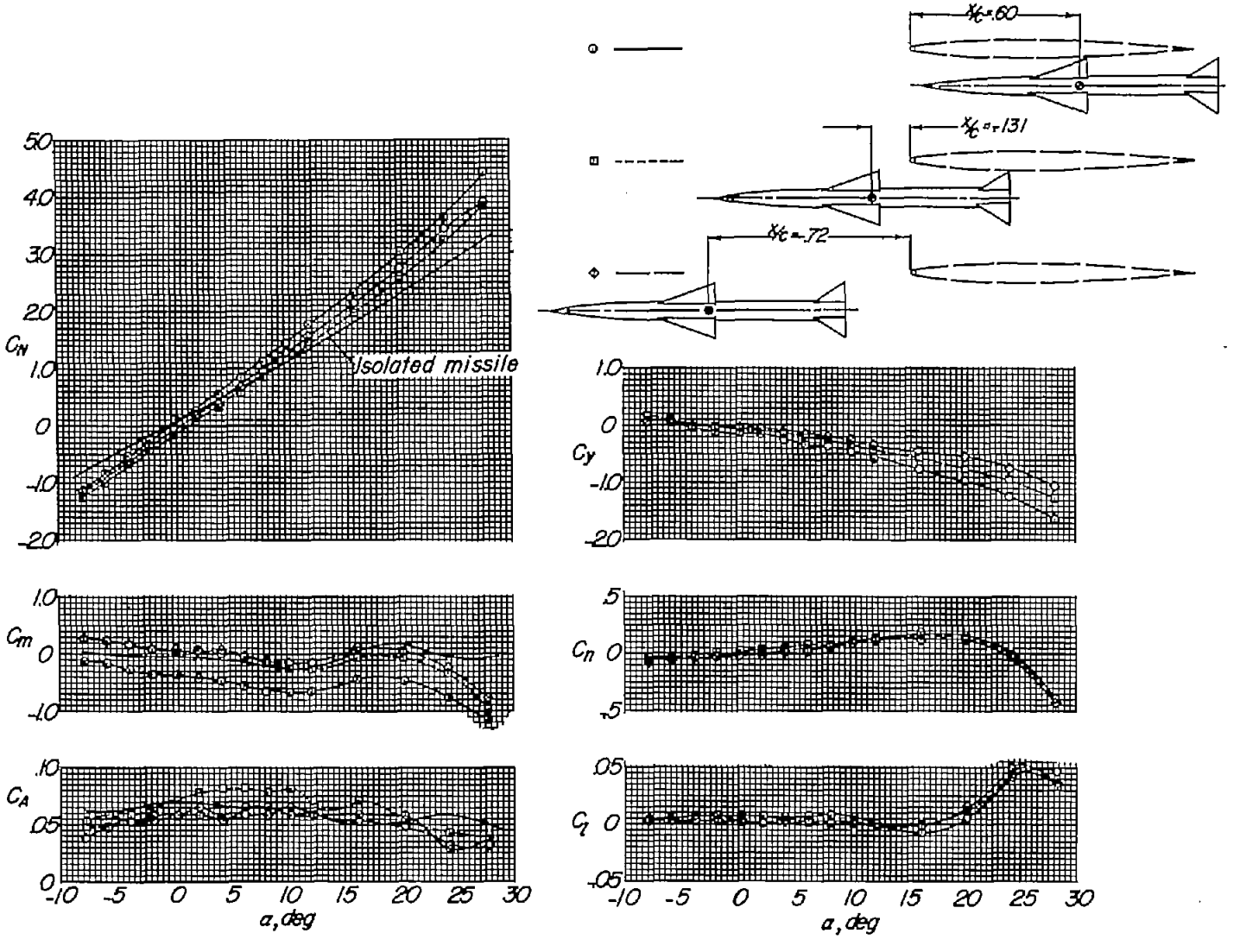

Figure 7.- Missile aerodynamic characteristics at the 25-percent-semispan station in the presence of the fuselage alone.

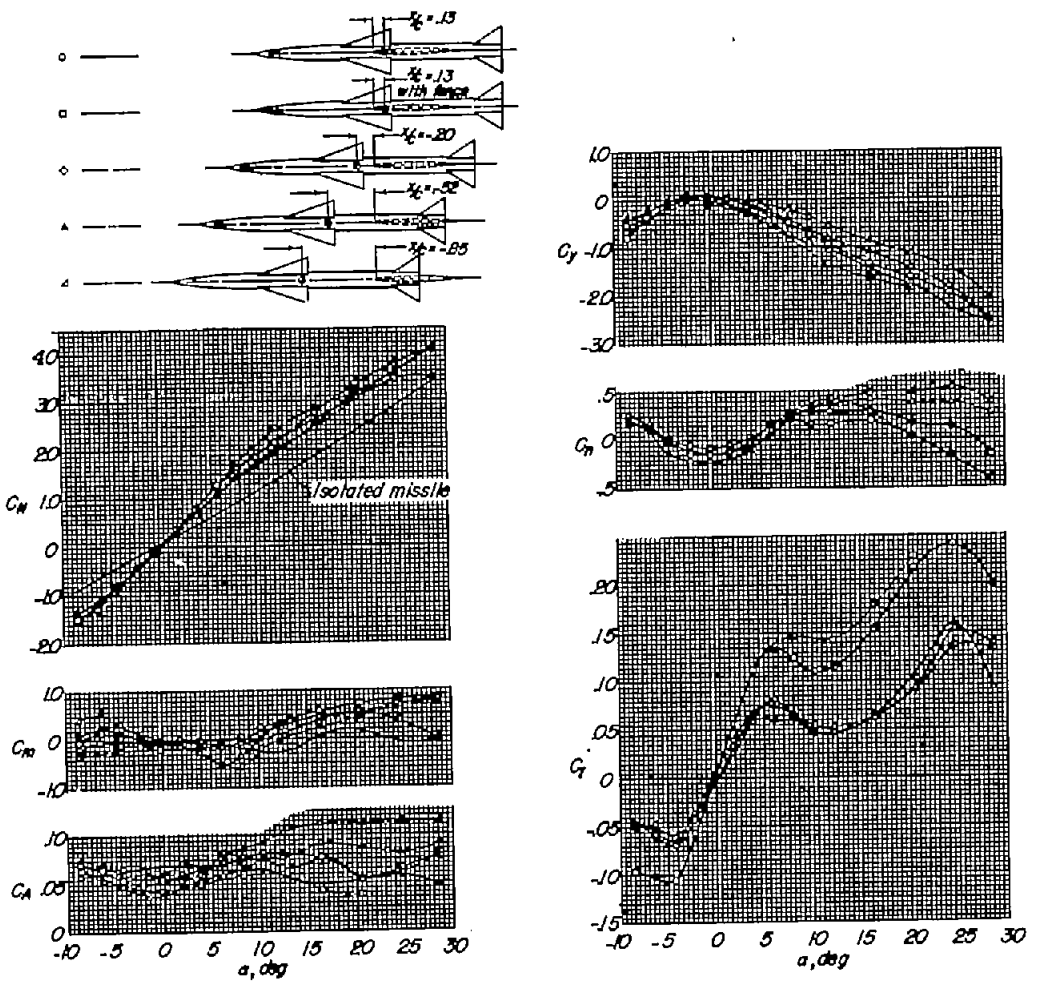

(a) x/c = 0.13 to x/c = -0.85.

Figure 8.- Missile aerodynamic forces and moments at the wing-tip location of the wing-fuselage combination.

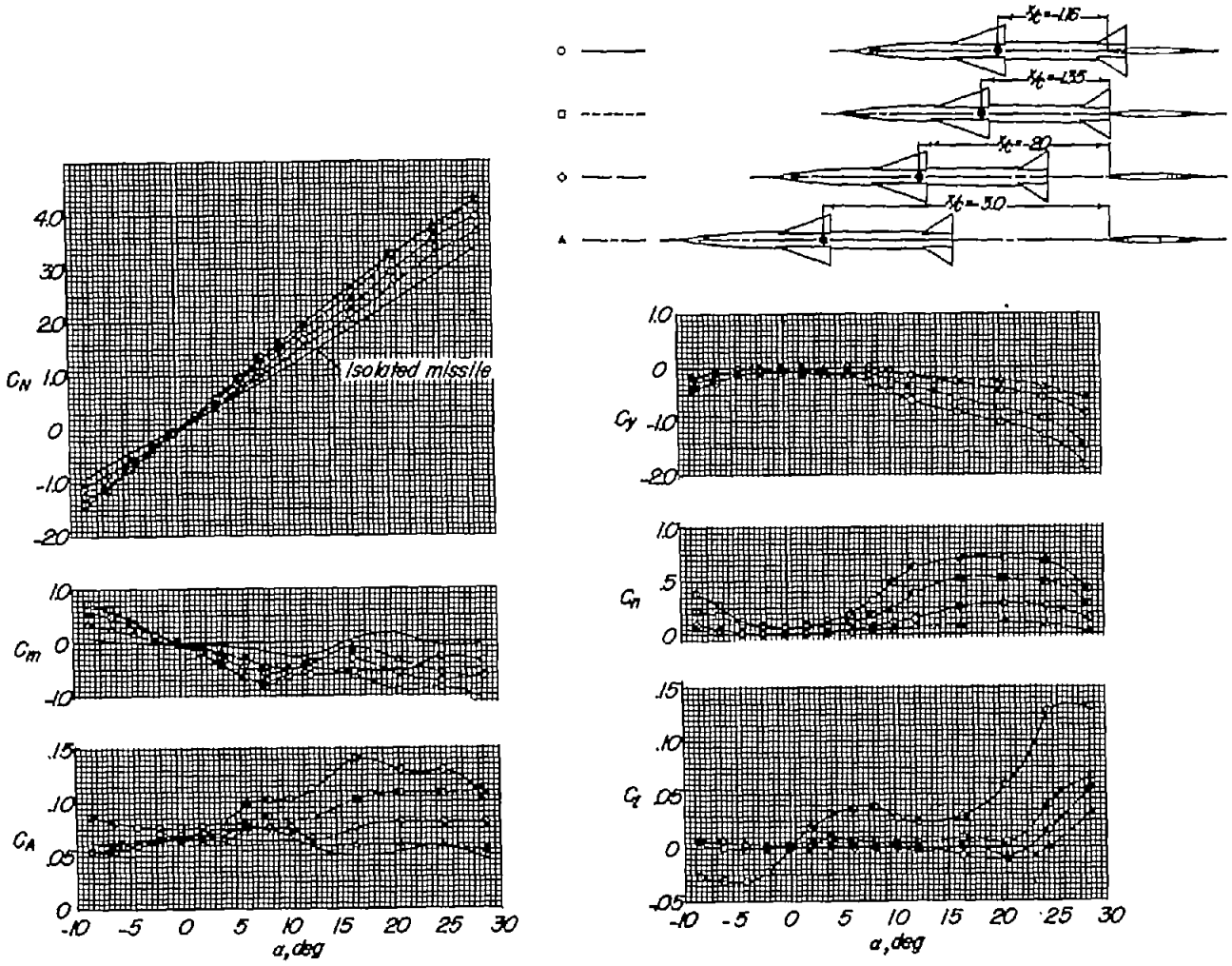

(b) x/c = -1.16 to x/c = -3.0.

Figure 8.- Concluded.

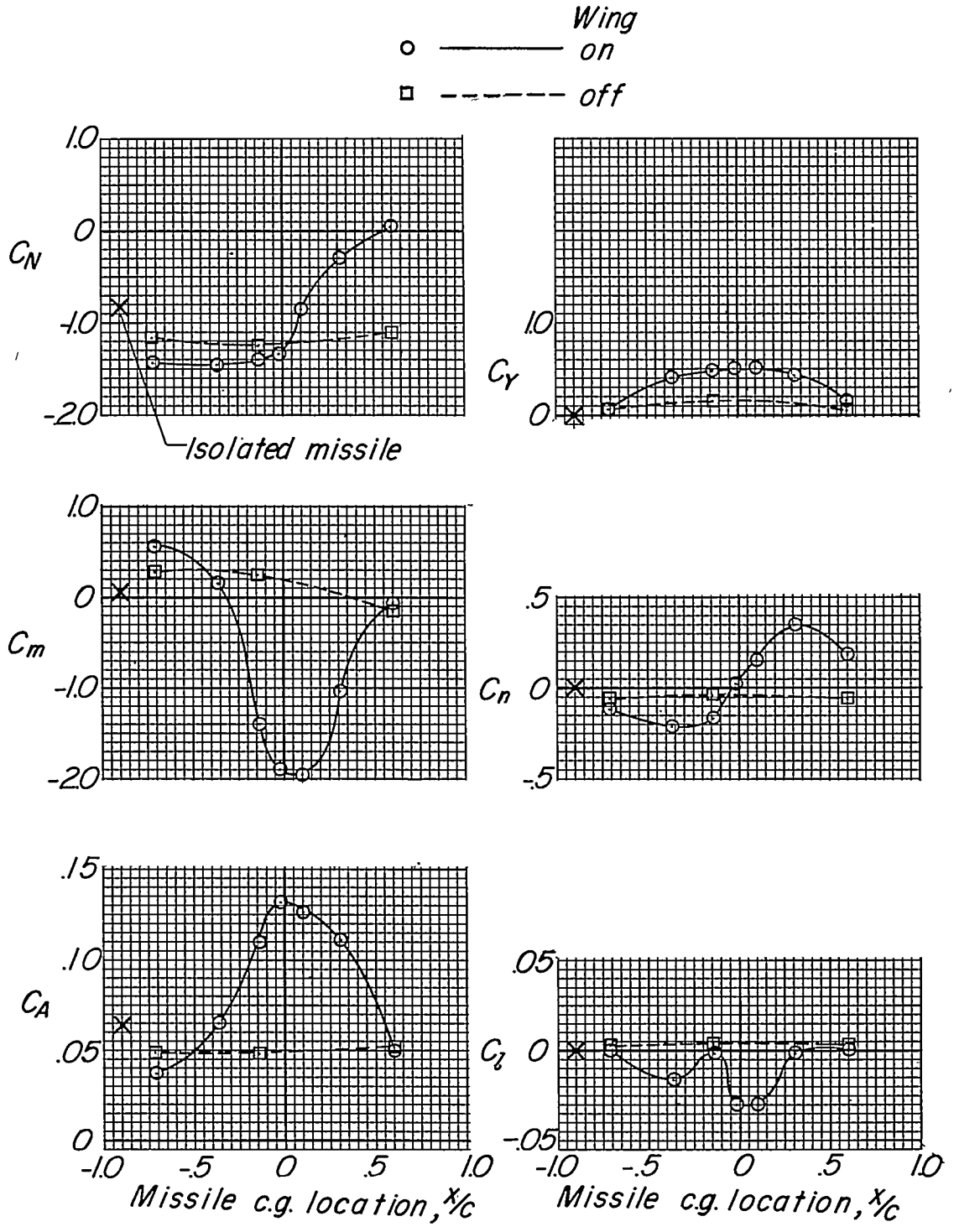

(a) $\alpha = -8^{\circ}$.

Figure 9.- Effect of chordwise position on missile forces and moments at the 25-percent-semispan location.

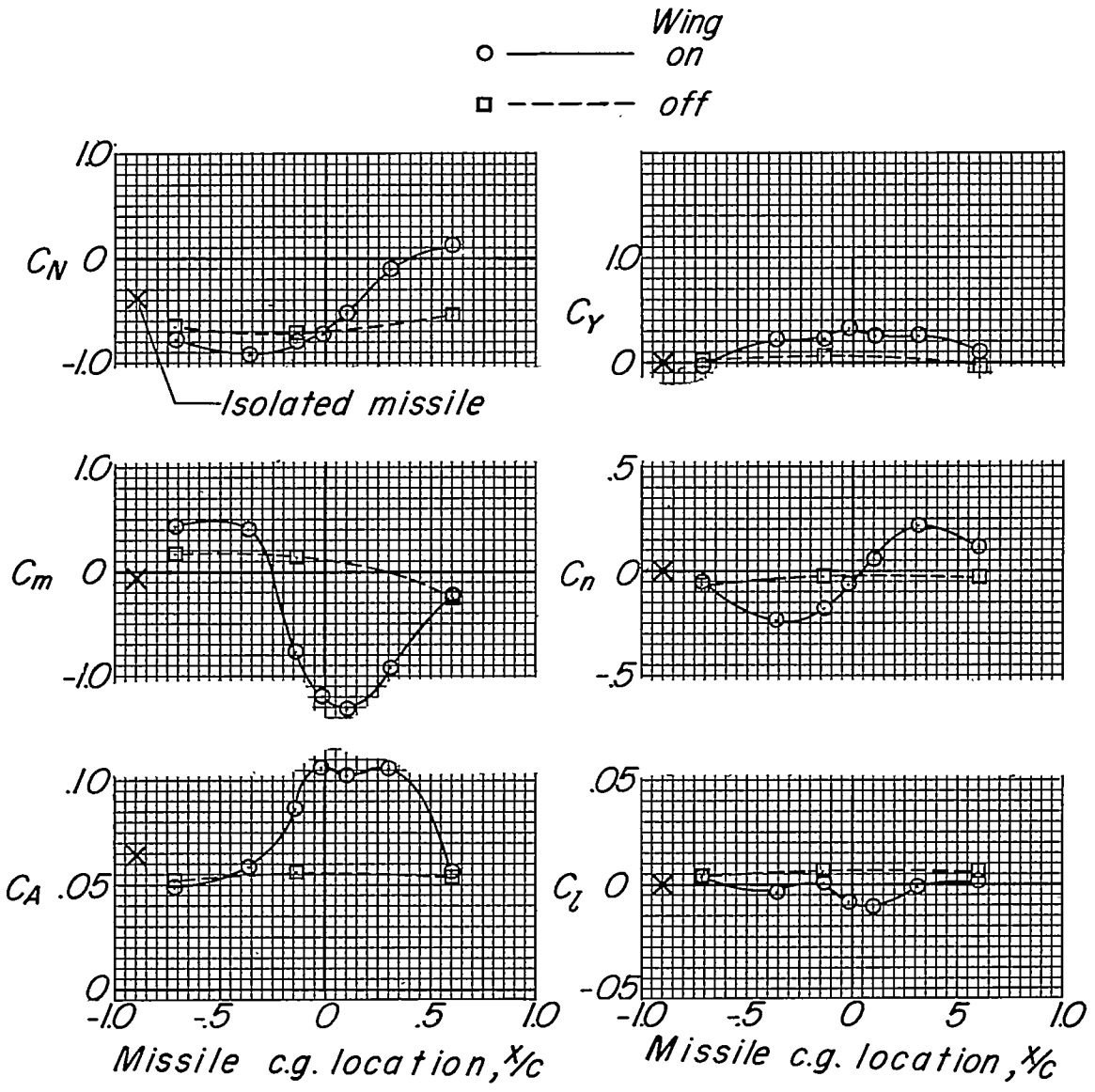

(b) $\alpha = -4^{\circ}$.

Figure 9.- Continued.

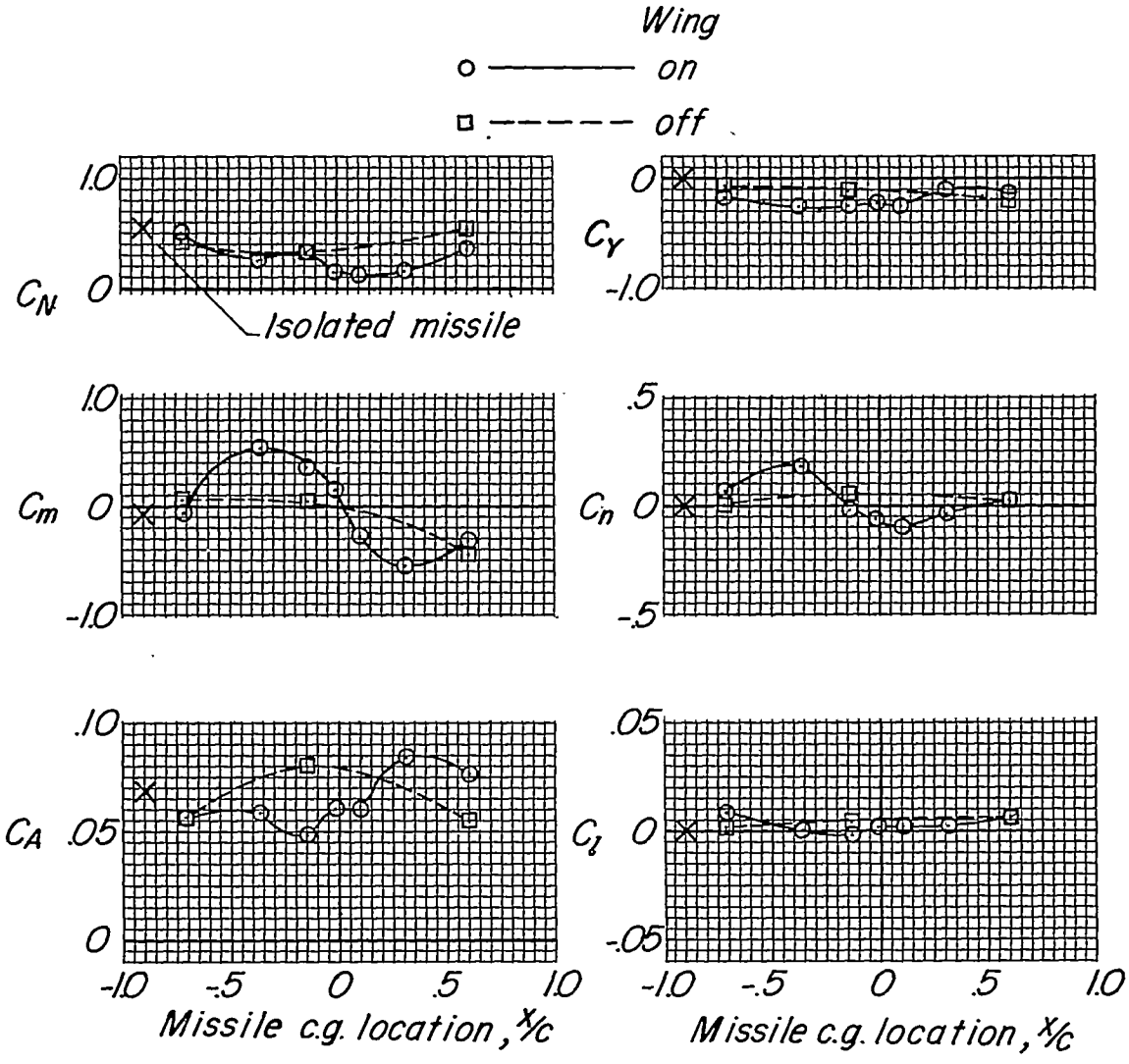

(d) $\alpha = 4^{\circ}$.

Figure 9.- Continued.

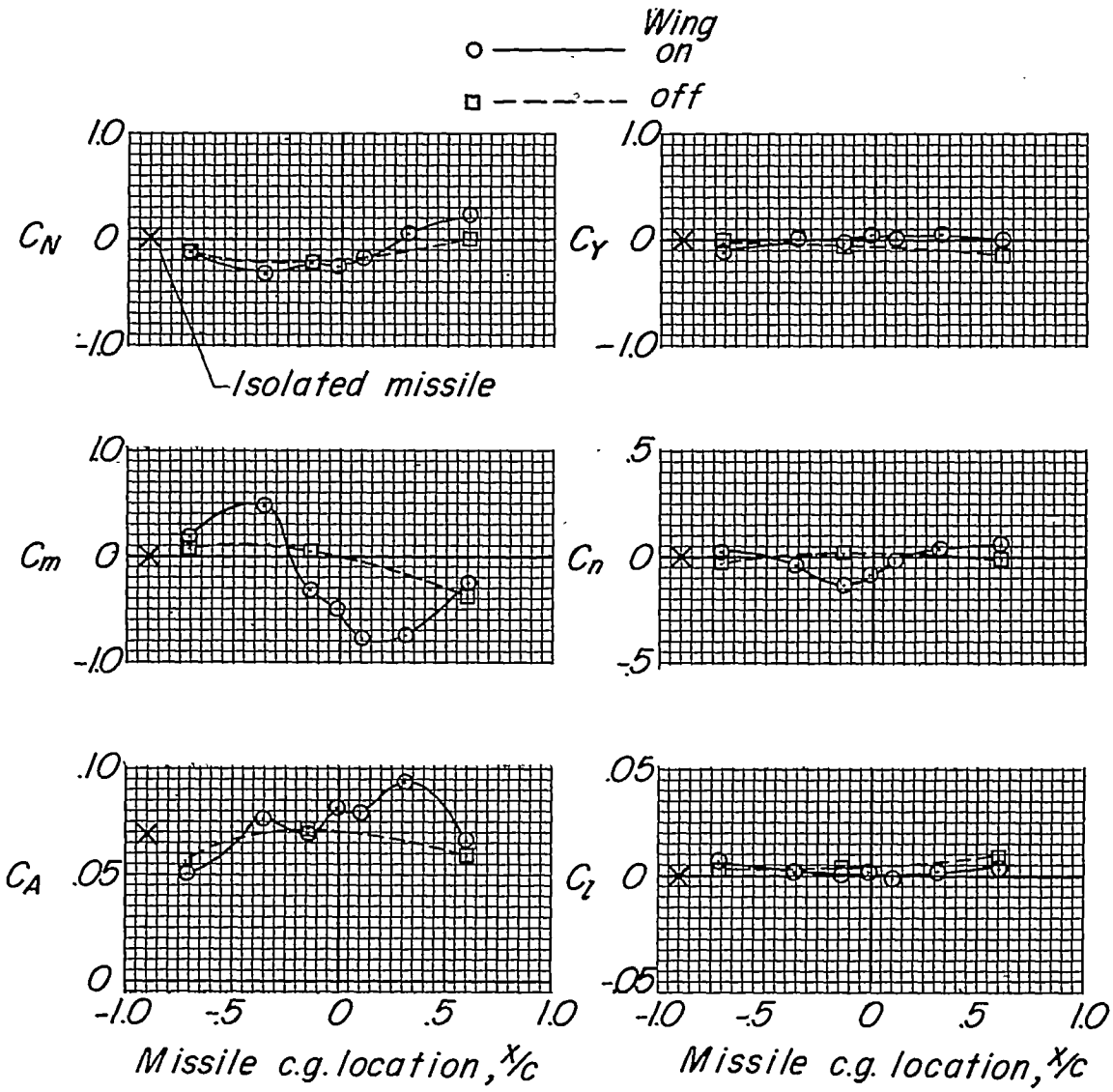

(c) $\alpha = 0^{\circ}$.

Figure 9.- Continued.

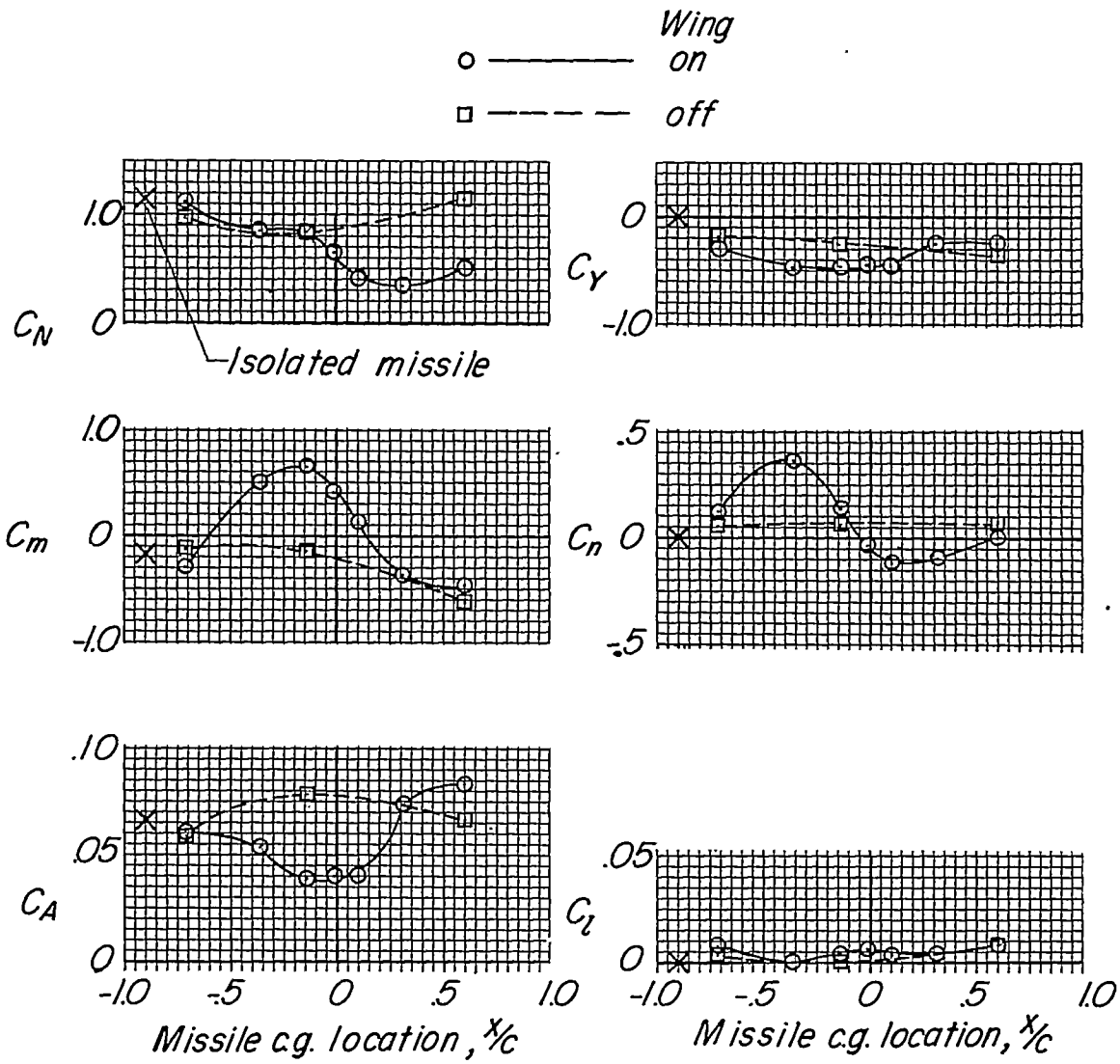

(e) $\alpha = 8^{\circ}$.

Figure 9.- Continued.

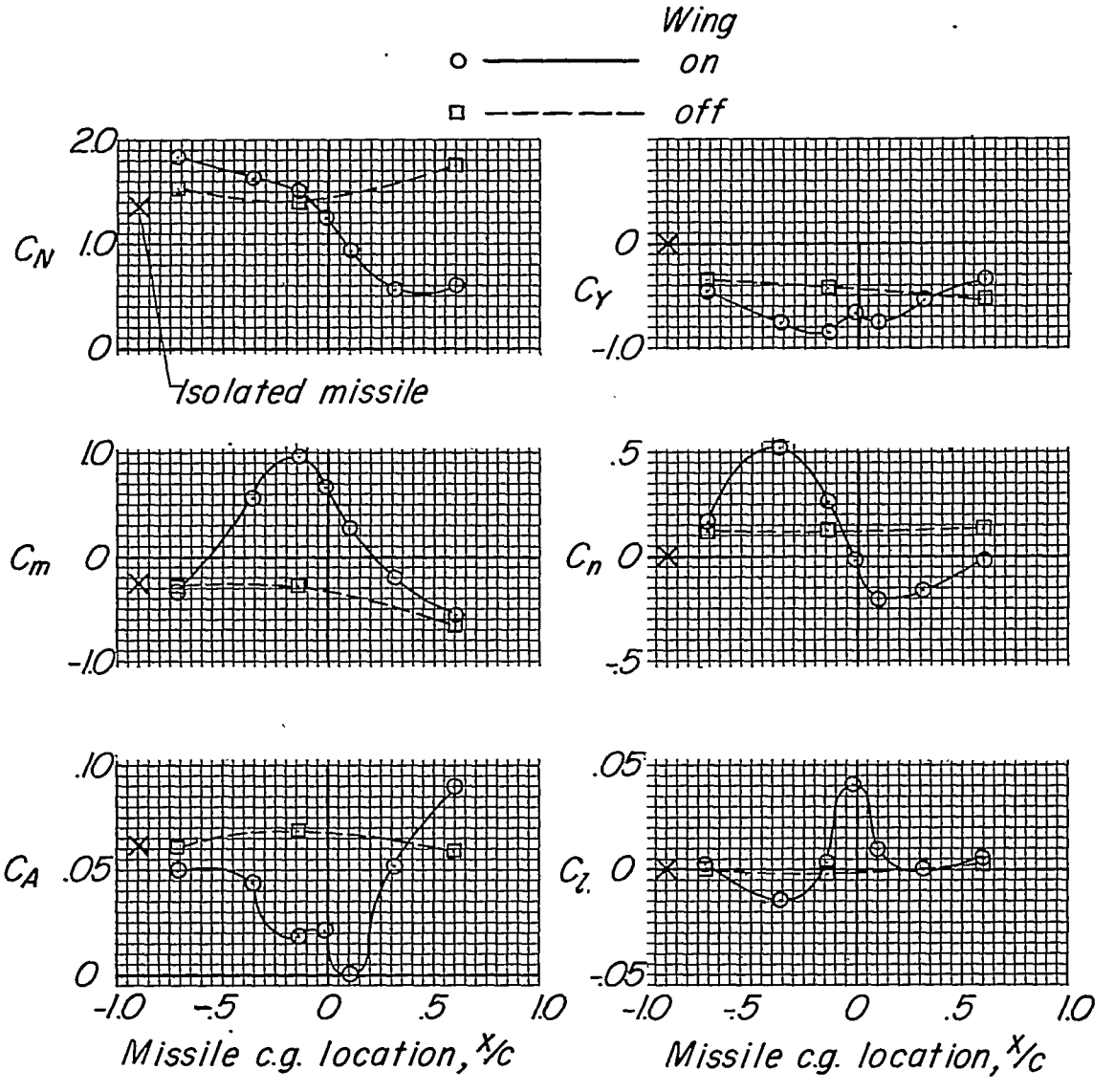

(f) $\alpha = 12^{\circ}$.

Figure 9.- Continued.

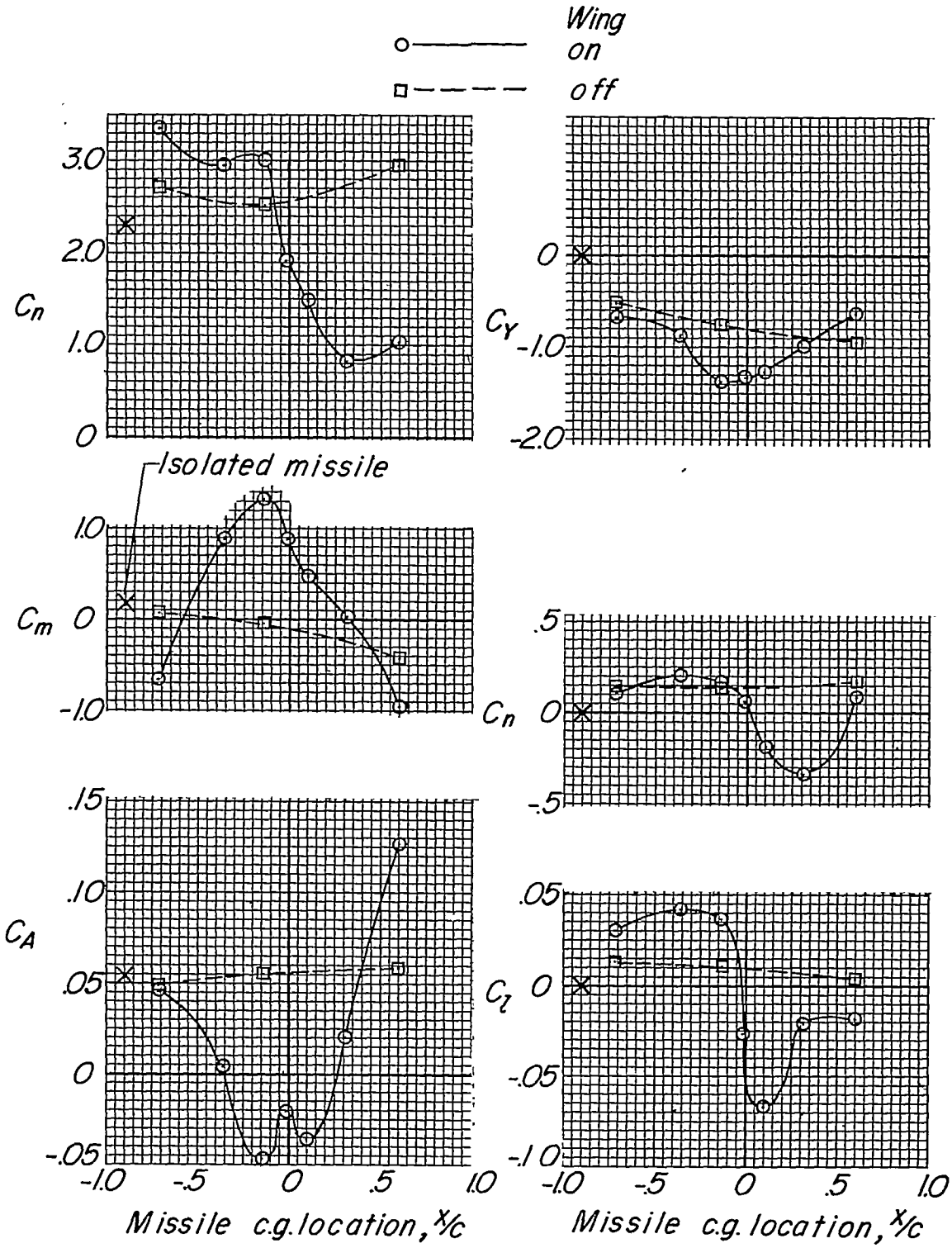

(g) $\alpha = 20^{\circ}$.

Figure 9.- Concluded.

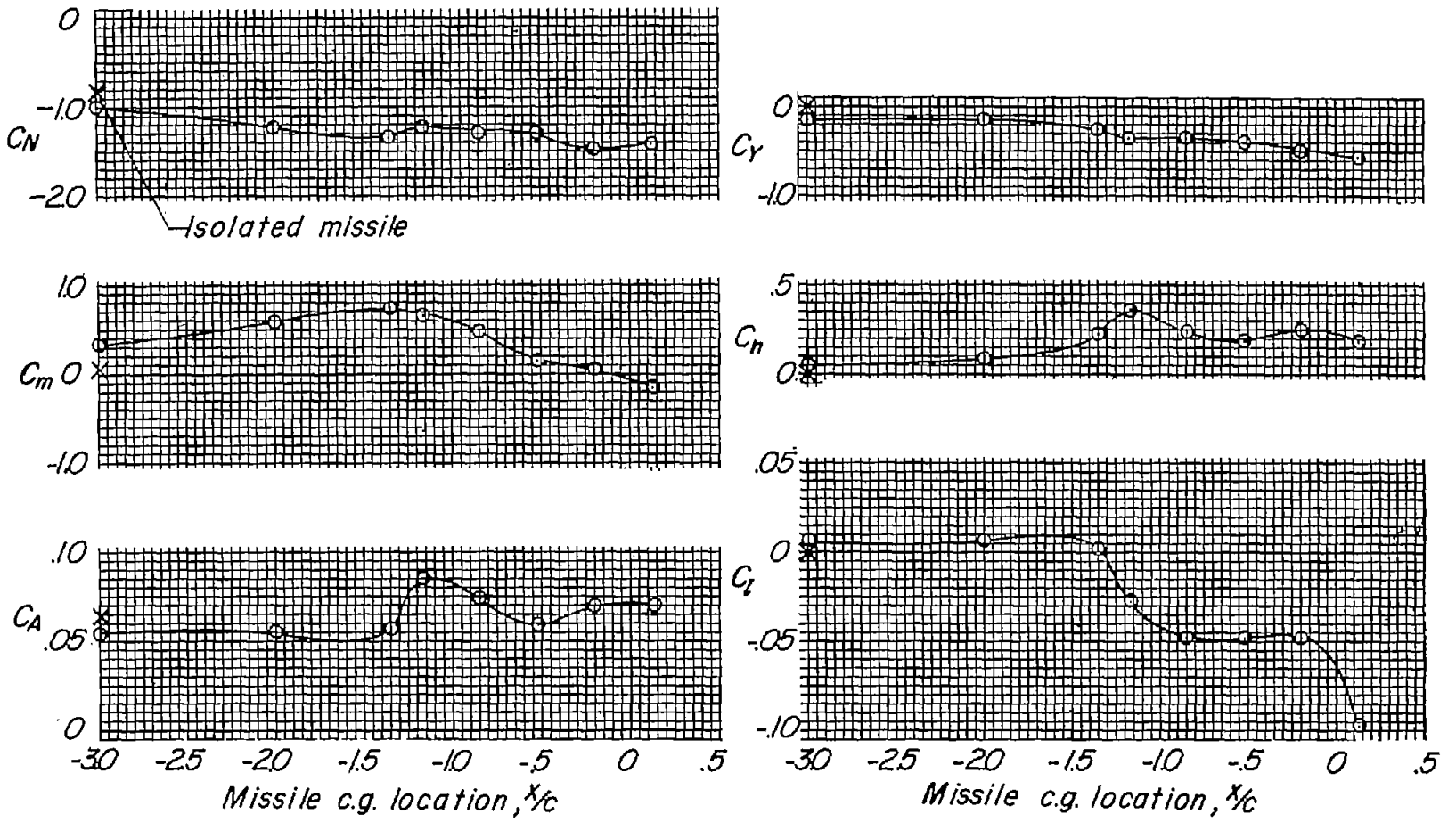

(a) $\alpha = -8^{\circ}$.

Figure 10.- Effect of chordwise position on the missile forces and moments at the wing-tip location.

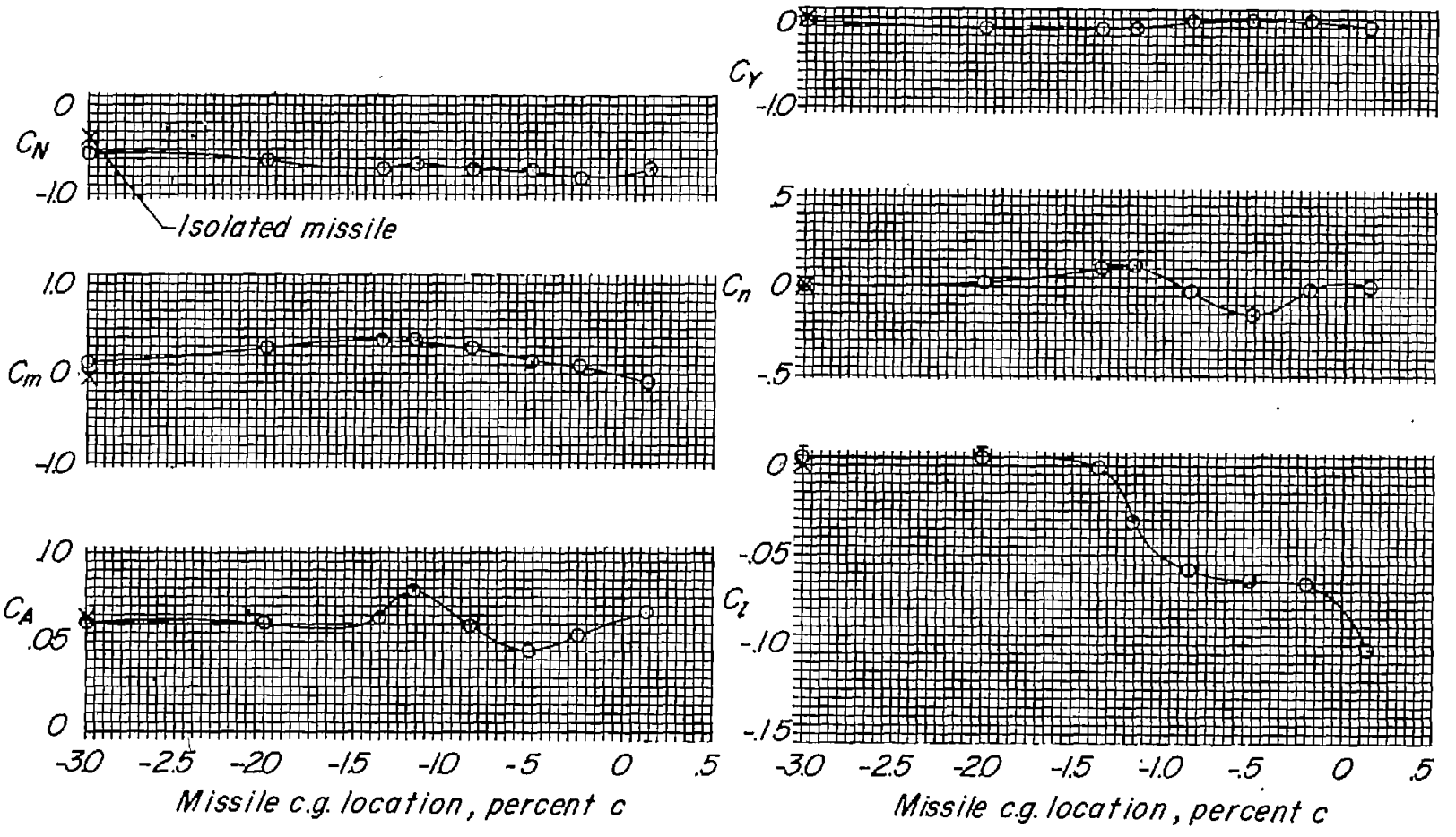

(b) $\alpha = -4^{\circ}$.

Figure 10.- Continued.

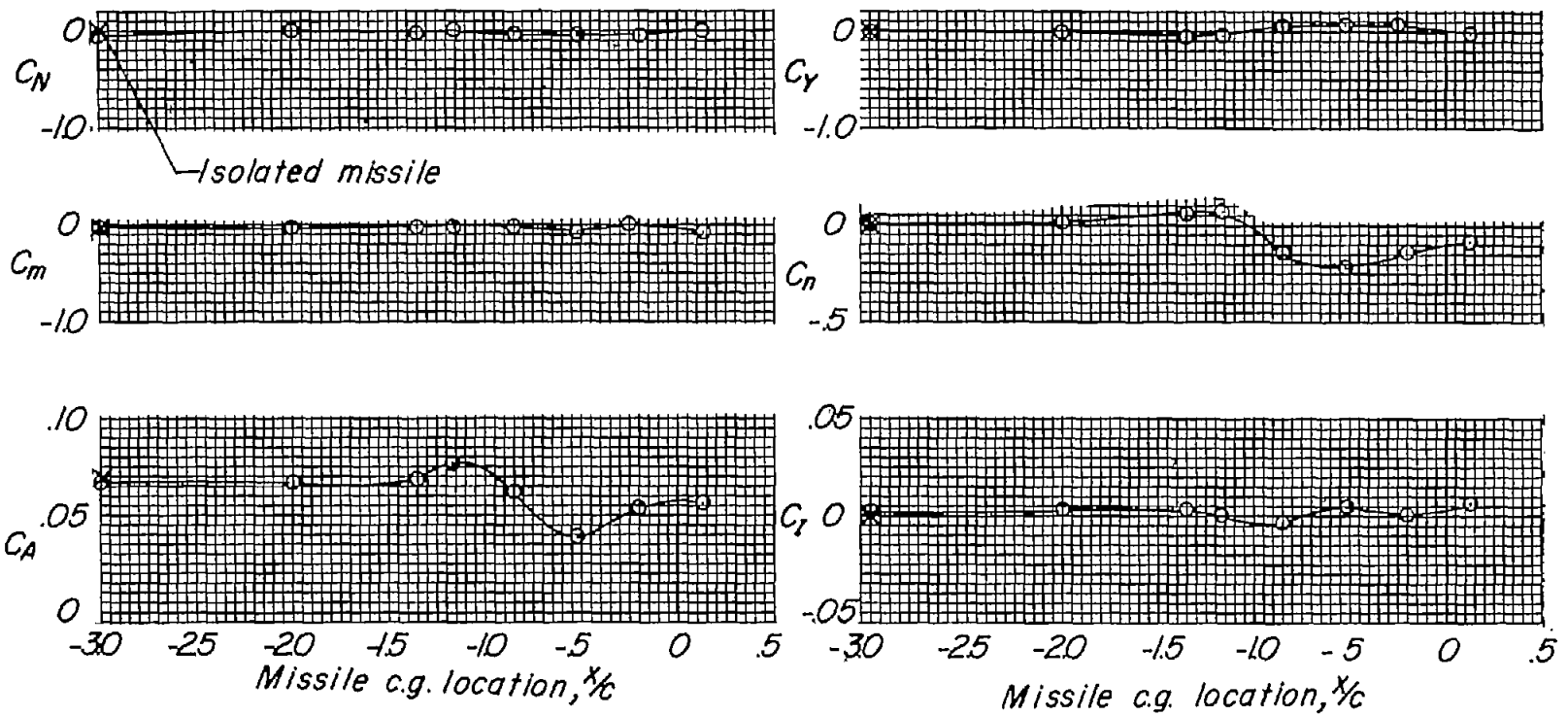

(c) $\alpha = 0^{\circ}$.

Figure 10.- Continued.

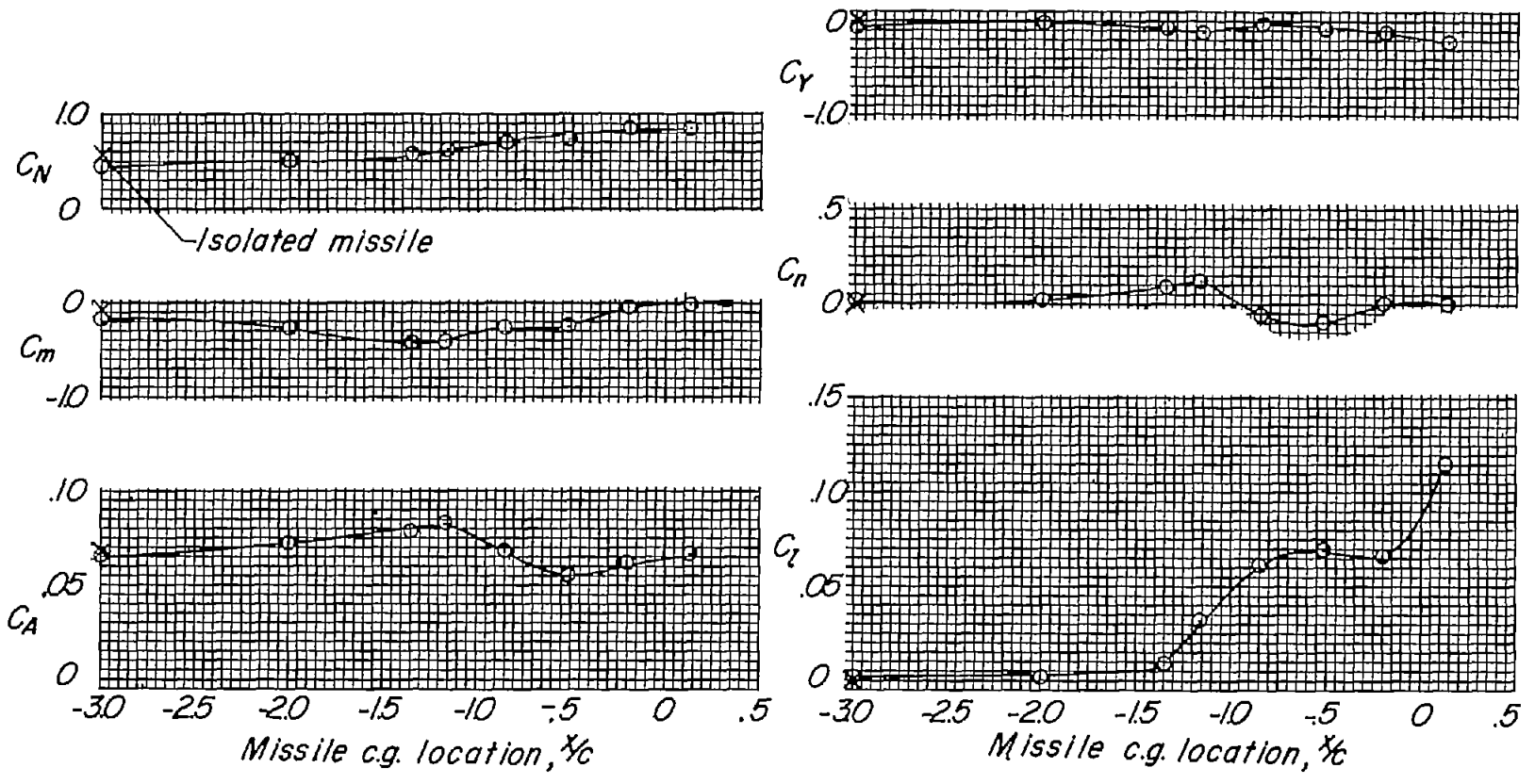

(d) $\alpha = 4^\circ$.

Figure 10.- Continued.

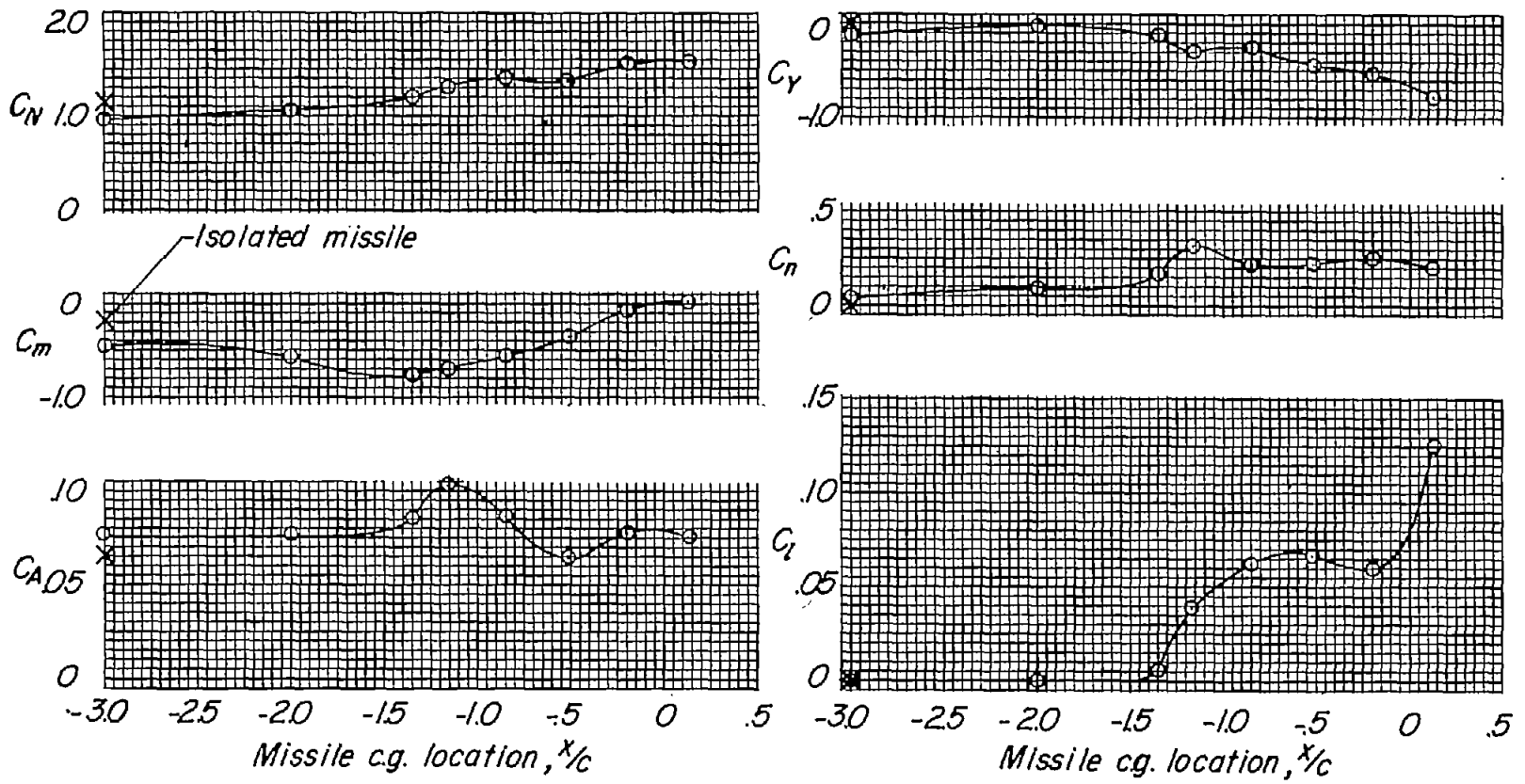

(e) $\alpha = 8^{\circ}$.

Figure 10.- Continued.

[redacted]

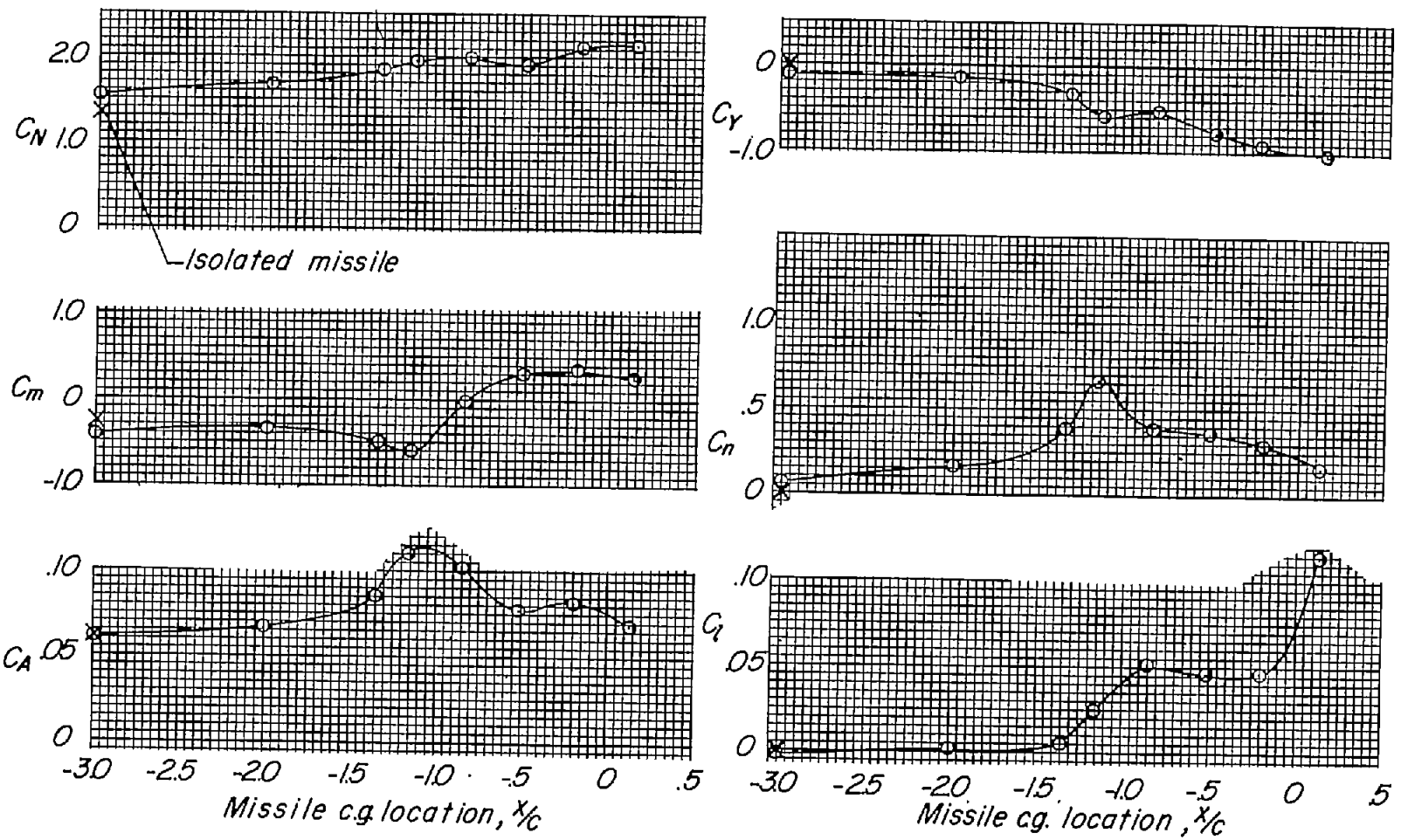

(f) $\alpha = 12^{\circ}$.

Figure 10.- Continued.

[redacted]

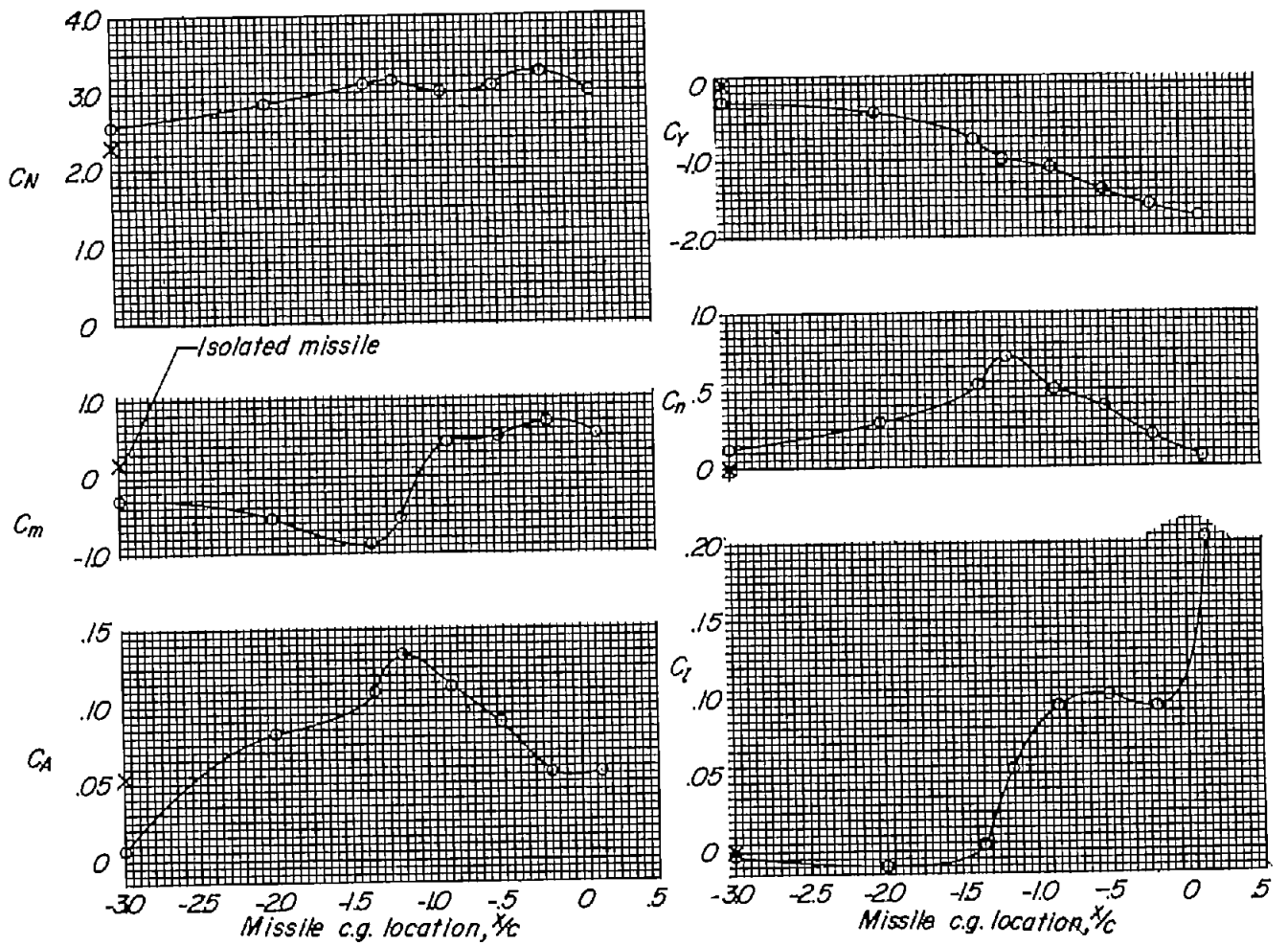

(g) $\alpha = 20^{\circ}$.

Figure 10.- Concluded.

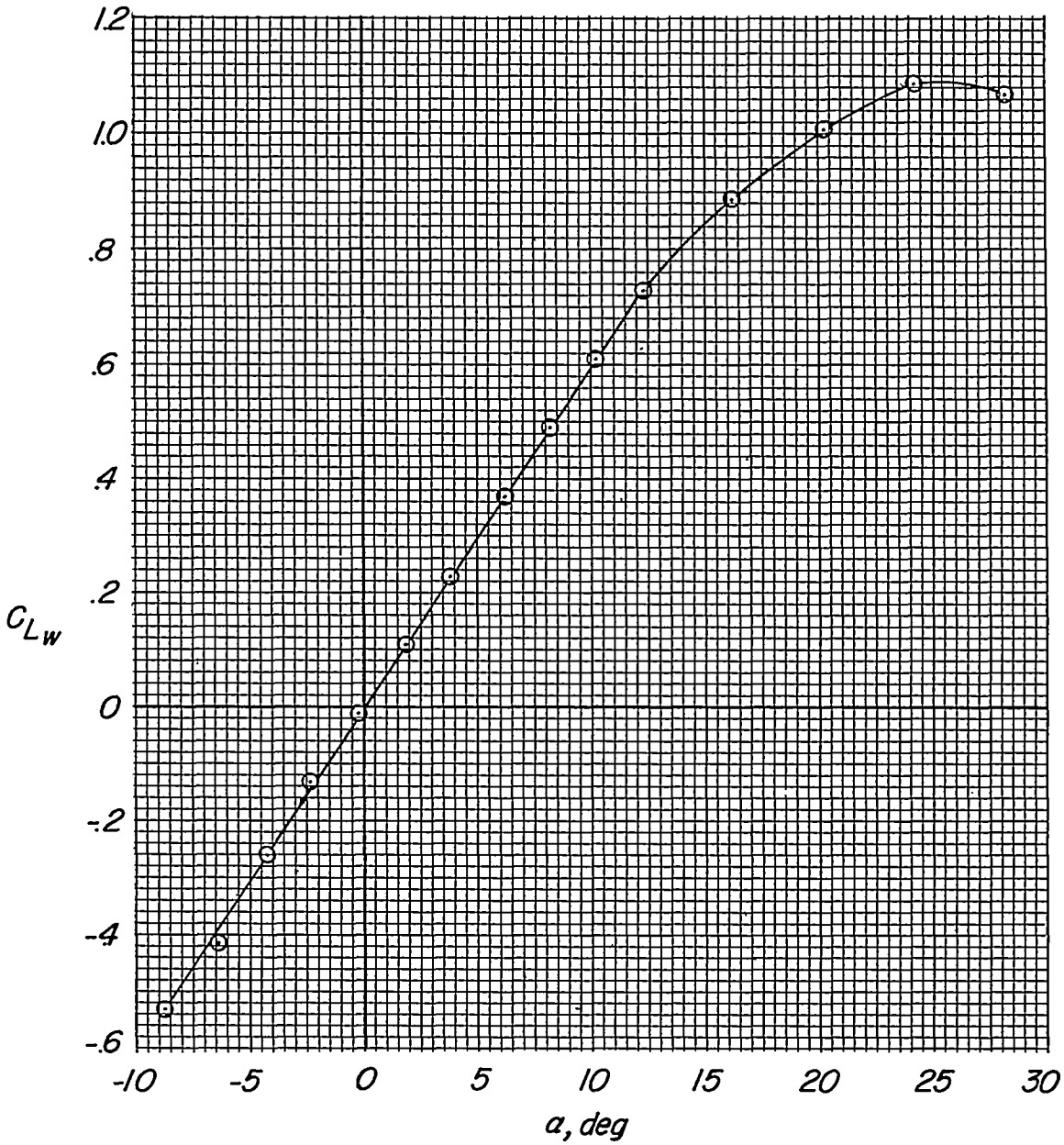

Figure 11.- Lift characteristics of the wing-fuselage combination.

NACA-Langley - 5-25-55 - 325